0-315-01207-2

National Library of Canada | Bibliothèque nationale du Canada

Canadian Theses Division | Division des thèses canadiennes

Ottawa, Canada K1A 0N4

49065

PERMISSION TO MICROFILM — AUTORISATION DE MICROFILMER

• Please print or type — Écrire en lettres moulées ou dactylographier

Full Name of Author — Nom complet de l'auteur

MONICA MARIJA PALCIC

Date of Birth — Date de naissance

Nov. 7 1950

Country of Birth — Lieu de naissance

Canada

Permanent Address — Résidence fixe

224 Charlotte
Hamilton, Ont
L8K 4V6

Title of Thesis — Titre de la thèse

Cyanide Binding and Compound I Formation of Human Erythrocyte Catalase

University — Université

University of Alberta

Degree for which thesis was presented — Grade pour lequel cette thèse fut présentée

Ph. D.

Year this degree conferred — Année d'obtention de ce grade

1980

Name of Supervisor — Nom du directeur de thèse

Dr. H.B. Dunford

Permission is hereby granted to the NATIONAL LIBRARY OF CANADA to microfilm this thesis and to lend or sell copies of the film.

The author reserves other publication rights, and neither the thesis nor extensive extracts from it may be printed or otherwise reproduced without the author's written permission.

L'autorisation est, par la présente, accordée à la BIBLIOTHÈQUE NATIONALE DU CANADA de microfilmer cette thèse et de prêter ou de vendre des exemplaires du film.

L'auteur se réserve les autres droits de publication; ni la thèse ni de longs extraits de celle-ci ne doivent être imprimés ou autrement reproduits sans l'autorisation écrite de l'auteur.

Date

May 16/1980

Signature

Monica Palcic

NL-91 (4/77)

National Library of Canada
Collections Development Branch

Canadian Theses on
Microfiche Service

Bibliothèque nationale du Canada
Direction du développement des collections

Service des thèses canadiennes
sur microfiche

NOTICE

The quality of this microfiche is heavily dependent upon the quality of the original thesis submitted for microfilming. Every effort has been made to ensure the highest quality of reproduction possible.

If pages are missing, contact the university which granted the degree.

Some pages may have indistinct print especially if the original pages were typed with a poor typewriter ribbon or if the university sent us a poor photocopy.

Previously copyrighted materials (journal articles, published tests, etc.) are not filmed.

Reproduction in full or in part of this film is governed by the Canadian Copyright Act, R.S.C. 1970, c. C-30. Please read the authorization forms which accompany this thesis.

THIS DISSERTATION HAS BEEN MICROFILMED EXACTLY AS RECEIVED

AVIS

La qualité de cette microfiche dépend grandement de la qualité de la thèse soumise au microfilmage. Nous avons tout fait pour assurer une qualité supérieure de reproduction.

S'il manque des pages, veuillez communiquer avec l'université qui a conféré le grade.

La qualité d'impression de certaines pages peut laisser à désirer, surtout si les pages originales ont été dactylographiées à l'aide d'un ruban usé ou si l'université nous a fait parvenir une photocopie de mauvaise qualité.

Les documents qui font déjà l'objet d'un droit d'auteur (articles de revue, examens publiés, etc.) ne sont pas microfilmés.

La reproduction, même partielle, de ce microfilm est soumise à la Loi canadienne sur le droit d'auteur, SRC 1970, c. C-30. Veuillez prendre connaissance des formules d'autorisation qui accompagnent cette thèse.

LA THÈSE A ÉTÉ MICROFILMÉE TELLE QUE NOUS L'AVONS REÇUE

Ottawa, Canada
K1A 0N4

NL-339 (Rev. 8/80)

THE UNIVERSITY OF ALBERTA

CYANIDE BINDING AND COMPOUND I FORMATION OF HUMAN ERYTHROCYTE CATALASE

by

MONICA MARIJA PALCIC

A THESIS

SUBMITTED TO THE FACULTY OF GRADUATE STUDIES AND RESEARCH

IN PARTIAL FULFILMENT OF THE REQUIREMENTS FOR THE DEGREE

OF DOCTOR OF PHILOSOPHY

DEPARTMENT OF CHEMISTRY

EDMONTON, ALBERTA

FALL, 1980

THE UNIVERSITY OF ALBERTA

FACULTY OF GRADUATE STUDIES AND RESEARCH

The undersigned certify that they have read, and recommend to the Faculty of Graduate Studies and Research, for acceptance, a thesis entitled Cyanide Binding and Compound I Formation of Human Erythrocyte Catalase submitted by Monica Marija Palcic in partial fulfilment of the requirements for the degree of Doctor of Philosophy in Chemistry.

H. S. Dunford
Supervisor

James W. Burns

Nella Rabenstein

B. Grant Kratochvil

R. W. Mitchell

W. Walker
External Examiner

Date May 14/90

ABSTRACT

The reaction of human erythrocyte catalase, with cyanide and hydroperoxides was investigated in hopes of obtaining more information about the active site of the enzyme. Stopped flow and rapid scanning techniques were used to study the formation of the primary oxidized compound (compound I) of catalase using peracetic acid, methyl hydroperoxide and ethyl hydroperoxide as substrates. The pH dependence of the apparent second order rate constants indicates that the process occurs by reaction of catalase with unionized hydroperoxide molecules. The pH independent rate constants for the formation of compound I follow a trend of decreasing rate as the size of the substrate increases.

Cyanide binding to catalase was studied using temperature jump and stopped flow techniques. The results are consistent with a mechanism in which HCN binds to the active site which contains no groups capable of ionization in the pH range of the study. The association equilibrium constant was determined from the relaxation amplitudes of the temperature jump experiments and by spectrophotometric titration.

The optical absorption and circular dichroic (CD) spectra of catalase and its cyanide, azide and fluoride derivates were also studied. The fractions of the protein

structure present as α-helix, β pleated sheet and unordered structure were estimated from the CD spectrum in the far ultraviolet region. The CD spectra also indicate that the protein conformation does not change appreciably after cyanide binding.

ACKNOWLEDGEMENTS

I would like to acknowledge the help of many people during the preparation of this thesis. Professor H.B. Dunford, my research director provided supervision, suggestions and interest throughout this work. Many valuable discussions were held with Drs. D. Job, H. Steiner and W.D. Hewson during their stays in the group. I would like to especially acknowledge the help of Drs. Tsune Araiso and Alex Nadezhdin and Ms. Libby Ralston who are not only my co-workers but my friends.

The expert assistance of the staff in the electronics, machine and glass shops is much appreciated. Finally I would like to thank Shirley Stawnychy for her skillful typing of this manuscript. Specific acknowledgements are made at the end of chapters.

TABLE OF CONTENTS

CHAPTER		PAGE
I	INTRODUCTION	1
	1.1 General Information	1
	1.2 Historical Background of Catalase	1
	1.3 Physical and Chemical Properties of Catalase	3
	1.4 References	8
II	SPECTRAL STUDIES OF HUMAN ERYTHROCYTE CATALASE	12
	2.1 Summary	12
	2.2 Introduction	12
	2.3 Experimental Procedures	13
	2.4 Results	21
	2.5 Discussion	29
	2.6 References	36
	2.7 Acknowledgments	40
III	THE REACTION OF HUMAN ERYTHROCYTE CATALASE WITH HYDROPEROXIDES TO FORM COMPOUND I	41
	3.1 Summary	41
	3.2 Introduction	42
	3.3 Experimental Procedures	43
	3.4 Results	46
	3.5 Discussion	59

3.6 References 65
3.7 Acknowledgments 67
3.8 Appendix 67
III KINETICS OF CYANIDE BINDING BY HUMAN ERYTHROCYTE CATALASE 68
4.1 Summary 68
4.2 Introduction 68
4.3 Experimental Procedures 69
4.4 Results 71
4.5 Discussion 89
4.6 References 92
4.7 Acknowledgments 93
Appendix I Carboxypeptidase A 94

List of Tables

Table	Description	Page
1.1	Kinetic Constants of Catalase Reactions with Hydrogen Peroxide	7
2.1	Absorption and Circular Dichroic Spectra of Human Erythrocyte Catalase Complexes	25
3.1	Wavelength Maxima and Extinction Coefficients of Optical Spectra of Human Erythrocyte Catalase and Compound I	49
3.2	Rate constants for the Formation of Compound I with Peracetic Acid	53
3.3	Rate Constants for the Formation of Compound I with Methyl Hydroperoxide	55
3.4	Compound I Formation	60
4.1	Data for the Binding of Cyanide by Catalase at 25°	73
4.2	Experimental Rate Constants from Stopped Flow Data at 25° and Ionic Strength 0.11	78
4.3	Parameters Obtained from Analysis of k_{1app}, k_{-1app} and K_{CN} vs. pH profiles for Cyanide Binding to Catalase	84
5.1	Activity of Metallocarboxypeptidases	99

List of Figures

Figure		Page
1.1	Structure of Ferriprotoporphyrin IX	5
2.1	SDS Disc Gel Electrophoresis of Human Erythrocyte Catalase	18
2.2	Circular Dichroism and Absorption Spectra of Human Erythrocyte Catalase in the Aromatic, Soret and Visible Regions; Native Enzyme, Cyanide and Azide Complexes	23
2.3	Circular Dichroism and Absorption Spectra of Human Erythrocyte Catalase in the Aromatic, Soret and Visible Regions; Native Enzyme and Fluoride Complex	26
2.4	Circular Dichroism Spectra of Acid and Alkaline Treated Catalase	27
2.5	Absorption Spectra of Acid and Alkaline Treated Catalase	28
2.6	Circular Dichroism Spectra in the Far Ultraviolet Region	30
2.7	First Derivative of the EPR Spectrum at 77°K of Native Human Erythrocyte Catalase and its Cyanide Derivative in 0.5 M Phosphate Buffer pH 7.0	31
3.1	Rapid Scan Spectrophotometric Measurements of Catalase with Methyl Hydroperoxide	47

3.2	Absorption Spectra of Native Catalase and Compound I in the Soret and Visible Regions	48
3.3	Plots of k_{obs}, the Pseudo First Order Rate Constant for Compound I Formation vs. [Peracetic Acid]	51
3.4	Plots of k_{obs}, the Pseudo First Order Rate Constant for Compound I Formation vs. [Methylhydroperoxide]	52
3.5	The pH Dependence of Compound I Formation with Peracetic Acid	57
3.6	The pH Dependence of Compound I Formation with Methyl Hydroperoxide	58
3.7	Plots of k_{obs}, the Pseudo First Order Rate Constant for Compound I Formation vs. [Ethyl Hydroperoxide]	61
4.1	Scatchard Plot of Cyanide Binding to Human Erythrocyte Catalase	72
4.2	Temperature Jump Relaxation of Catalase-Cyanide at pH 9.06	76
4.3	Concentration Dependence of Reciprocal Relaxation Time against Equilibrium Concentration of Cyanide and Enzyme at Various pH Values	77
4.4	Stopped Flow Kinetics of Cyanide Binding to Catalase at various pH Values	79

4.5	The pH Dependence of k_{1app}	81
4.6	The pH Dependence of k_{-1app}	82
4.7	Relaxation Amplitudes as a Function of Total Cyanide, $(CN)^{o}$	86
4.8	The pH Dependence of K_{CN}	88
5.1	The (Partly) Non-Productively Bound Complex of a Dipeptide and Carboxypeptidase A	97

LIST OF ABBREVIATIONS

CD	Circular Dichroism
EPR	Electron Paramagnetic Resonance
MCD	Magnetic Circular Dichroism
SDS	Sodium Dodecyl Sulfate

CHAPTER I.

INTRODUCTION

1.1 General Introduction

During the period of the author's research, four separate projects on the enzyme catalase were completed. They are the isolation and purification of catalase from human erythrocyte cells, a study of erythrocyte catalase spectral properties, its reactions with hydroperoxides to form compound I and a study of cyanide binding to the enzyme. They are organized into three chapters in the thesis. Each chapter is intended to be complete with regard to an introduction, experimental section, results, and discussion. In addition there is an appendix on the enzyme carboxypeptidase A, a zinc containing hydrolytic enzyme.

1.2 Historical Background of Catalase

Catalases are enzymes that promote the catalatic reaction:

$$2\,H_2O_2 \longrightarrow 2\,H_2O + O_2 \qquad (1)$$

They were first reported by Thénard (1) who described the H_2O_2-cleaving activity of various tissues in 1819. Loew (2) introduced the term catalase and Warburg (3) identified iron as the metal ion of the active group of the enzyme.

Catalase was at the centre of intensive discussions

concerning the action of metals in biological oxidations in the 1920's and 1930's. Weiland (4) regarded the function of redox catalysts to be the activation of substrate hydrogen, which now finds its expression in our views of dehydrogenases, and assumed, in the initial redox reaction, hydrogen is transferred to oxygen to form peroxide. The role of metal ions was to remove the peroxide formed and the "catalase function" was as shown in equations 2,3:

$$H_2O_2 + \text{catalyst} \longrightarrow O_2 + \text{catalyst}\cdot 2H \qquad (2)$$

$$H_2O_2 + \text{catalyst}\cdot 2H \longrightarrow 2\ H_2O + \text{catalyst} \qquad (3)$$

Warburg (5) did not believe that hydrogen peroxide was formed during biological oxidations, but thought that iron of the cell activated oxygen to react directly with substrates, a view consistent with present ideas on oxygenation mechanisms (6). Like Willstätter, who also doubted the function of iron in peroxidases (7), he did not relate the catalatic reactions to the metal content of the enzyme. But after Zeile and Hellström prepared more concentrated catalase from liver and demonstrated its hematin nature (8), analogies between catalase and other hematin compounds were soon recognized. Stern (9) identified protohemin IX as the prosthetic group of the enzyme and it was one of the first enzymes to be isolated in a high state of purity (8). Its crystallization in 1937 from beef liver extracts

by Sumner and Dounce ranked among the early triumphs of biochemistry (10). Such studies opened the way to a systematic examination of the physical properties of catalase and led to the discovery, spectroscopic description and kinetic evaluation of its catalytic intermediates, compounds I and II.

In 1936 Stern (11) observed that the brown color of a catalase solution changed to a red color upon the addition of ethyl hydroperoxide. Using fast reaction techniques, pioneered by Hartridge and Roughton (12), Chance discovered that the red compound is preceded by a labile green compound (13), in a manner analogous to that of horseradish peroxidase reported earlier by Theorell (14). The two intermediates compound I, the labile green species and compound II, the red, are responsible for the catalatic and peroxidatic activity of catalase. Chance (15) erroneously considered compound I to be an enzyme-substrate complex as defined by Michaelis and Menten, (16) but this was disproved by George (17) who was able to form peroxidase compound I with potassium chloriridate and other oxidizing agents.

1.3 Physical and Chemical Properties of Catalase

Catalase isolated from most sources has a molecular weight of 240,000 and consists of four identical subunits each with a weight of 60,000. There are four ferriproto-

porphyrin IX groups per molecule of catalase, one on each subunit. Ferriprotoporphyrin IX (Fig. 1) is the prosthetic group found in other metalloproteins with very diverse biochemical functions, including hemoglobin, myoglobin and peroxidases.

Catalase is widely distributed in mammalian and non-mammalian aerobic cells and with a few exceptions it is lacking only in strict anaerobes (18). Although catalase is present in plant cells most workers have chosen to isolate the enzyme from bacterial and mammalian sources where it is present in high concentrations, i.e., *Micrococcus lysodeikticus*, liver and erythrocytes. Catalases from horse and bovine liver contain less than four hemin groups per molecule and this is probably due to some hemin being degraded to bile pigments (19).

A number of ligands, (including cyanide, fluoride, formate, acetate and azide (20),) bind to catalase to form spectroscopically and magnetically distinct derivatives. Unlike peroxidase, metmyoglobin and methemoglobin (21-23) catalase does not form alkaline derivatives (21). No native catalase can be reduced to the ferrous form by dighionite, and the maintenance of the protein structure depends on the presence of hemin. The amino acid sequence of bovine liver catalase has been reported (24).

Catalase exhibits both catalatic and peroxidatic activity. The catalatic reaction involves two steps:

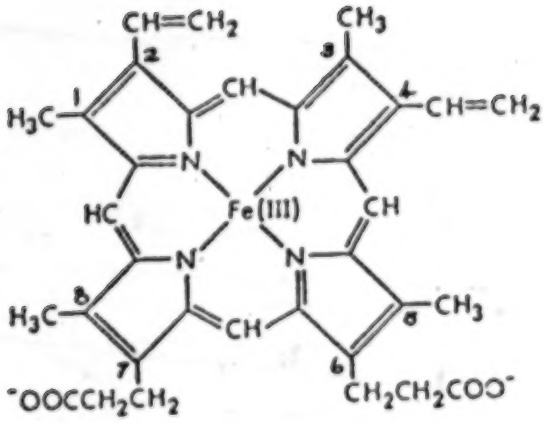

Fig. 1.1 Structure of Ferriprotoporphyrin IX.

$$\text{Native ferric catalase} + H_2O_2 \xrightarrow{k_1} \text{Compound I} + H_2O \quad (4)$$

$$\text{Compound I} + H_2O_2 \xrightarrow{k_2} \text{ferric catalase} + O_2 + H_2O \quad (5)$$

Values for k_1 and k_2 for catalase isolated from different sources are shown in Table 1.1. The oxygen evolved in equation 5 originates from intact O-O bonds in hydrogen peroxide (25).

Compound I can react with one or two electron donors to form Compound II or native enzyme. The rate of peroxidatic activity, equations 6, 7:

$$\text{Compound I} + AH \longrightarrow \text{Compound II} + A\cdot \quad (6)$$

$$\text{Compound II} + AH \longrightarrow \text{Ferric catalase} + A\cdot \quad (7)$$

is much lower in catalase than peroxidases.

Suitable electron donors for reaction 4 are ascorbate, ferrocyanide and phenols, for reaction 5 ascorbate and ferrocyanide (30). In addition catalase compound I can react with alcohols and formate to give native enzyme in a two-electron reduction reaction. The oxidation of ethanol to acetaldehyde by bovine liver catalase and hydrogen peroxide was shown to be stereospecific (31).

Neither the molecular geometry nor the electronic configuration of the iron porphyrin moiety in either compound I or II is known, their formal oxidation states are Fe V

Table 1.1 Kinetic constants of catalase reactions with hydrogen peroxide.

Catalase Source	k_1 x 10^{-7} $M^{-1}s^{-1}$	k_2 x 10^{-7} $M^{-1}s^{-1}$	Reference
Bacterial (M. lysodiecticus)	1	1.6	(26)
Horse Erythrocyte	0.4	1.8	(27)
Beef Liver	0.30	0.56	(28)
Beef Liver	0.15	3.0	(27)
Rat Liver	1.7	2.6	(29)

and Fe IV respectively. A discussion of the nature of compound I is found in chapter III.

The physiological function of catalase is unclear and it was once suggested that it is a "fossil enzyme" at least in higher animals (20). It seems clear however that catalase has a general function in detoxification of oxygen metabolites, although many details remain to be clarified (32). Hydrogen peroxide is produced by a number of enzymatic reactions occurring in living organisms, i.e., by oxidases and superoxide dismutase. A number of the hydrogen peroxide producing oxidases are found in the peroxisomes of liver cells where catalase is localized (29). Compound I formation in cells has been demonstrated by spectrophotometry of perfused rat liver; compound II has not been detected in cells (29).

A number of reviews of catalase have recently appeared on the molecular and catalatic properties (18,33,34) on catalase biosynthesis (32) and the biochemistry of peroxisomes (29). For more specific information these reviews should be consulted.

1.4 References

1. Thénard, L.J. (1819) Ann. Chim. Phys. 11, 85-87.
2. Loew, O. (1901) U.S. Dept. Agr. Rept. No. 68.
3. Warburg, O. (1923) Biochem. Z. 136, 266-277.

4. Weiland, H. (1932) On the Mechanisms of Oxidation Silliman Lectures, Yale University Press, New Haven.

5. Warburg, O. (1949) Heavy Metal Prosthetic Groups and Enzyme Action (Lawson, A. trans.) Oxford University Press, London.

6. Hayaishi, O. (1963) in "The Enzymes", Vol. 8, (Boyer, P.D., Lardy, H. and Myrböck, K. eds.) pp. 353-371, Academic Press, New York.

7. Willstätter, R. (1922) Chem. Ber. 55, 3601-3623.

8. Zeile, K. and Hellström, H. (1930) Hoppe-Seyler's Z. Physiol. Chem. 192, 171-192.

9. Stern, K.G. (1936) J. Biol. Chem. 112, 661-669.

10. Sumner, J.B. and Dounce, A.L. (1937) J. Biol. Chem. 121, 417-424.

11. Stern, K.G. (1936) J. Biol. Chem. 114, 473-494.

12. Hartridge, H. and Roughton, F.J.W. (1923) Proc. Roy. Soc. London, A 104, 376-394.

13. Chance, B. (1947) Acta Chem. Scand. 1, 236-237.

14. Theorell, H. (1941) Enzymologia 12, 250-252.

15. Chance, B. (1952) Arch. Biochem. Biophys. 41, 416-424.

16. Michaelis, L. and Menten, M.L. (1913) Biochem. Z. 49, 336-369.

17. George, P. (1953) Science, 220-221.

18. Deisseroth, A. and Dounce, A.L. (1970) Physiol. Rev. 50, 319-375.

19. Lemberg, R. and Legge, J.W. (1943) Biochem. J. 37, 117-127.

20. Nicholls, P. and Schonbaum, G.R. (1963) in "The Enzymes" 2nd ed. Vol. 8 (Boyer, P.D., Lardy, H. and Mybäck, K. eds.) pp. 147-225, Academic Press, New York.

21. Keilin, D. and Hartree, E.F. (1951) Biochem. J. 49, 88-104.

22. George, P. and Hanania, G. (1952) Biochem. J. 52, 517-523.

23. George, P. and Hanania, G. (1953) Biochem. J. 55, 236-243.

24. Schroeder, W.A., Shelton, J.R., Shelton, J.B., Robberson, B. and Appell, G. (1969) Arch. Biochem. Biophys. 131, 653-655.

25. Jarnagin, R.C. and Wang, J.H. (1958) J. Amer. Chem. Soc. 80, 786-787.

26. Stother, G.K. and Ackerman, E. (1961) Biochim. Biophys. Acta 47, 317-326.

27. Chance, B., Greenstein, D.S. and Roughton, F.J.W. (1952) Arch. Biochem. Biophys. 37, 301-321.

28. Zidoni, E. and Kremer, M.L. (1974) Arch. Biochem. Biophys. 161, 658-664.

29. Sies, H. (1974) Angew. Chem. Internat. Edit. 13, 706-718.

30. Keilen, D. and Nicholls, P. (1958) Biochim. Biophys. Acta 29, 302-307.

31. Corrall, R.J.M., Rodman, H.M., Margolis, J. and Landau, B.R. (1974) J. Biol. Chem. 249, 3181-3182.

32. Ruis, H. (1979) Can. J. Biochem. 57, 1122-1130.

33. Chance, B. and Schonbaum, G.R. (1976) in "The Enzymes", Vol. 13, Part C, (Boyer, P.D. ed.) pp. 363-408, Academic Press, New York.

34. Hewson, W.D. and Hager, L.P. (1979) in "The Porphyrins", Vol. VII. (Dolphin, D. ed.) pp. 295-332, Academic Press, New York.

CHAPTER II.

SPECTRAL STUDIES OF HUMAN ERYTHROCYTE CATALASE

2.1 Summary

The optical absorption and circular dichroic (CD) spectra of human erythrocyte catalase (EC 1.11.1.6) and its cyanide, azide and fluoride derivatives over the wavelength range of 210 to 700 nm are reported. Treatment with acid or alkali solutions causes spectral changes which may be due to dissociation of the enzyme into subunits and removal of the heme group from the protein. The fractions of the protein structure present as α-helix, β pleated sheet and unordered structure have been estimated from the CD spectrum in the far ultraviolet region. The CD spectra also indicate that the protein conformation does not change appreciably after cyanide binding. EPR spectroscopy of the native enzyme and its cyanide complex are reported. The spectral results are compared to catalase obtained from other mammalian and bacterial sources.

2.2 Introduction

Human erythrocyte catalase (EC1.11.1.6, hydrogen-peroxide: hydrogen-peroxide oxidoreductase) is a ferric hemoprotein which has been isolated in pure form (1-5) and partially characterized. It contains four intact heme groups and is present in relatively large amounts in

whole blood, about 300 mg/ℓ. The physicochemical properties which have been studied include isoelectric point, sedimentation coefficients, molecular weight, amino acid content, EPR and NMR spectra (3-7). Circular dichroism (CD) studies are useful probes in obtaining information on the secondary and tertiary structures of proteins in solution and on conformational changes which accompany ligand binding and denaturation (8). However, no CD studies of human erythrocyte catalase have been reported as yet. This chapter describes studies on the circular dichroism and absorption spectra of human erythrocyte catalase and its cyanide, fluoride and azide derivatives and the EPR spectra of the native enzyme and its cyanide complex. The conformational changes with denaturants such as acid and alkali are also reported.

2.3 Experimental Procedures

The isolation procedure followed is a method developed by Aebi and coworkers (5) with modifications suggested by Bonaventura *et al*. (4). The preparation consists of nine steps;

i) isolation and washing of red blood cells
ii) hemolysis
iii) desalting of hemolysate using dialysis
iv) batch adsorption of catalase on DEAE cellulose
v) washing of resin and desorption of enzyme

vi) concentration by ultrafiltration or ammonium sulfate precipitation

vii) chromatography on CM cellulose

viii) chromatography on Sephadex G-150 or LKB AcA22 Ultrogel

ix) concentration by vacuum dialysis or ultrafiltration

Two pints of 21-day-old blood or fresh blood samples preserved in a solution containing citrate, phosphate and dextrose commonly called CPD are used for the isolation. Sixty three ml of CPD is added to each unit as an anticoagulent and antihemolysant. The whole blood is centrifuged at 4°, 4000 X g for 20 min and the plasma and buffy layer (white blood cells and lipids) are removed by aspiration from the packed red blood cells. The cells are washed three times with four volumes of cold isotonic saline solution (0.9% NaCl). For each wash the cells are suspended in saline, centrifuged 13,200 X g, 20 minutes, and the supernatant is decanted.

The packed cells are hemolyzed by adding an equal volume of cold distilled deionized water and stirring gently for 1 h at 4°. The hemolysate is centrifuged 20 min, 13,200 Xg at 4° to remove stromata, i.e., the cell membranes, yielding a supernatant liquid which is dialyzed overnight against distilled water at 4° to lower the ionic strength of the solution for batchwise adsorption on DEAE cellulose. One hundred and seventy five g of Whatman DE-52 is equilibrated with 1.5 mM phosphate buffer pH 6.8. The dialyzed

hemolysate is added to equilibrated DEAE in the ratio of 0.5 volumes of settled DEAE to 1 volume of packed cells. The resin does not have the capacity to adsorb even a fraction of the hemoglobin present since the concentration of hemoglobin in adult males is 16 ± 2 g/100 ml of whole blood (9), whereas the capacity of Whatman DE-52 is 850 mg (Insulin)/g dry resin. Further, hemoglobin with an isoelectric point (pI) of 6.9 is slightly positively charged at pH 6.8 while catalase (pI 6.1 (3), 5.8 (10)) has a net negative charge. DE-52 has a net positive charge from pH 3 to pH 9 and will adsorb catalase completely and hemoglobin slightly at low ionic strength. Care must be taken in this step to ensure that the ionic strength of the resin and dialyzed hemolysate is low; the specific conductance of the solution should be at least 0.30 mmho. If adsorption of enzyme to resin is not complete[1] after 1 h an equal volume of distilled deionized water should be added to lower the ionic strength of the solution. When adsorption of catalase to the resin is complete the resin is washed in a large Buchner funnel with 1.5 mM phosphate buffer pH 6.8, to get rid of most of the remaining hemoglobin. Next the resin is packed in a 6.5 x 60 cm column, and four liters of 1.5 mM phosphate buffer, pH 6.8 are run through the column. The eluent containing hemoglobin is discarded. Catalase is desorbed by passing 20 mM phosphate buffer, pH 6.8, through the

[1]Adsorption is complete when there is no activity in supernatant solution above resin. Activity measurements carried out as described on page 19.

column. Fifteen ml fractions are collected and those containing 10% of the activity of the tube with maximum enzyme activity are combined and concentrated in a 200 ml Amicon ultrafiltration cell with an XM-50 membrane. Concentration can also be carried out by ammonium sulfate precipitation of the pooled fractions. Solid ammonium sulfate to 35% saturation (11) is added to the fractions after 0.1 volume of 1M phosphate buffer pH 7.0 is added. After 3 hr of slow stirring, a tan precipitate is centrifuged off and discarded. The solution is brought to 40% saturation, stirred overnight and centrifuged. The red supernatant fluid is discarded.

The dark green precipitate is dissolved in 100 mM acetate buffer, pH 4.8 and adsorbed on a column 2.5 x 14 cm packed with Whatman CM-52 resin previously equilibrated with 100 mM acetate buffer, pH 4.8. The column is developed using a linear pH gradient consisting of 1000 ml of 100 mM acetate buffer pH 4.8 to 1000 ml 50 mM phosphate buffer pH 6.8. Catalase elutes in a volume of 200 ml starting at 1500 ml in the gradient. Its desorption is often preceded by an unidentified "yellow band". Hemoglobin does not desorb and is effectively removed from catalase in this step.

In order to eliminate traces of contaminating proteins a 1.5 x 90 cm Sephadex G-200 column is used. Sephadex G-200 has a fractionation range of 10,000-500,000 molecular

weight and catalase is eluted before contaminating proteins. LKB AcA22 Ultrogel with a fractionation range 100,000-1,200,000 has also been used in later preparations. 3 ml fractions are collected and active fractions pooled and concentrated to at least 10 mg/ml (12) on a vacuum dialyzer or 50 ml Amicon ultrafiltration cell with an XM-50 membrane. The concentrated solution is then dialyzed into pH 7.0 buffer with an ionic strength of 0.05 prepared from quintuply distilled water (13). The concentrated enzyme is kept at 4° until needed.

The following precautions not mentioned above should be taken. Rubber gloves should be worn when handling whole blood samples; there is a danger of developing some "non-specific" infection. Neither whole blood nor catalase should be frozen; red cells lyse and catalase denatures after freezing (14). Before sample is added to dialysis tubing, the tubing should be checked for pinholes by filling with water.

Seventeen enzyme isolations were carried out during the author's research. The RZ (Reinheitszahl) value, the ratio of absorbance at 405 nm and 275 nm is most often used as a measure of purity of a catalase preparation, and should be greater than 1.2. The purity of such preparation is greater than 95% (5) as seen by SDS disc gel electrophoresis, Fig. (2.1). Ultracentrifugal analysis was carried out on a Beckman Model E ultracentrifuge using a

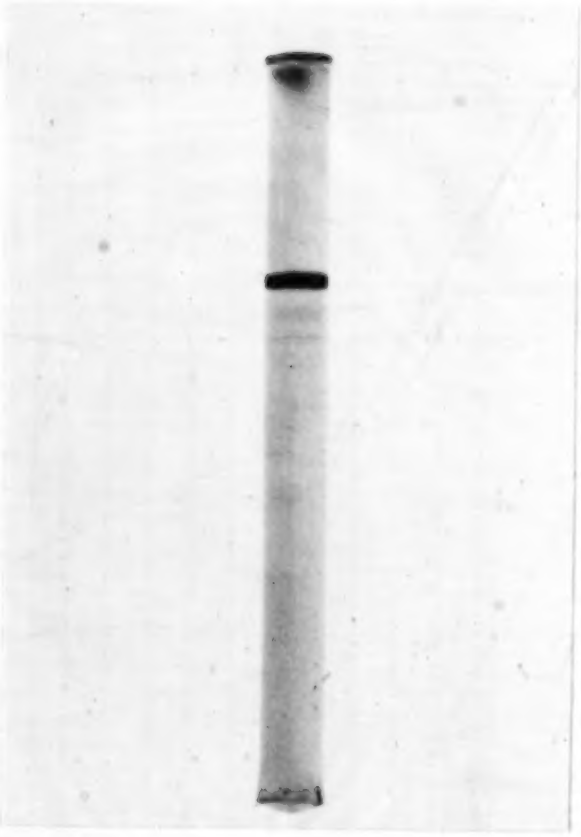

Fig. (2.1) SDS disc gel electrophoresis of Human Erythrocyte catalase. Electrophoresis was carried out on 25 µg of enzyme as described by Porzio and Pearson (17); 10% acrylamide gels, 1 ma per tube, 7 hr, Coomassie Blue Stain.

uv scanner, at 20° in 0.05 M phosphate buffer pH 6.6. The sedimentation velocity pattern showed a single boundary, and $S_w^{20} = 10.5$. Low speed sedimentation equilibrium centrifugation for 52 h at 20°, $\omega = 5600$, assuming a partial specific volume of 0.724 (3), gave a weight average molecular weight of 225,000 which did not vary over the cell (15). Catalase is obtained in approximately a 40% yield, about 130 mg of enzyme from two pints of whole blood.

Catalase activity is measured by a modification of the method of Beers and Sizer (16) in which the disappearance of hydrogen peroxide with time is followed spectrophotometrically at 240 nm. In the assay 2.6 ml of 0.05 M phosphate buffer, pH 6.8 and 0.3 ml of stock substrate solution are added to a 3 ml cuvette and absorbance at 240 nm noted. A measured amount, 1-5 µl, of solution to be assayed is added to the cuvette on a paddle and the change in absorbance is recorded for up to 30 s. The decrease in absorbance (which is equal to $-\frac{d[H_2O_2]}{dt}$) is determined from the slope of the best-fit line drawn through the recorder line. The observed rate constant is calculated using equation (1):

$$-\frac{d[H_2O_2]}{dt} = k_{obs}\,[H_2O_2] \qquad (1)$$

The concentration of catalase [E] is determined spectrophotometrically at 405 nm using a molar extinction coefficient of $3.97 \times 10^5\ M^{-1}cm^{-1}$ (4). Specific activity is expressed as $k_{obs}/[E]$ and should be greater than 3.4×10^7

$M^{-1}s^{-1}$. There were four unsuccessful preparations with an RZ $\leq$ 1. These were used for preliminary measurements. Other isolations had RZ values of 1.15 to 1.29. One preparation with an RZ value of 1.13 was used for CD and some preliminary kinetic measurements and had identical properties to enzyme with an RZ of 1.27. All studies used enzyme from at least two and usually three preparations and the results obtained from different preparations did not vary. Typical specific activity values are 3.5×10^7 $M^{-1}s^{-1}$ for RZ 1.27, 3.6×10^7 $M^{-1}s^{-1}$ for RZ 1.13 and 3.6×10^7 $M^{-1}s^{-1}$ for RZ 1.20 enzyme.

For spectral studies the azide and cyanide derivatives were prepared by the addition of KCN, KF and NaN_3 to a final concentration of 0.1 mM cyanide and 100 mM fluoride and azide. Denaturation was performed by adjusting the pH with dilute HCl or NaOH. Unless otherwise noted, all spectra were obtained in phosphate buffer with an ionic strength of 0.05 and pH 7.0 at 25°C. Quintuply distilled water was used for preparing all solutions. All chemicals used were of reagent grade.

The measurements of CD were carried out with a Jasco model ORD/UV-5 spectrophotometer equipped with a CD attachment. The instrument had been calibrated with an aqueous solution of d-10-camphorsulfonic acid (Eastman Kodak). The cells were 20 mm in length and jacketed so they could be thermostated to 25°C. Below 250 nm a 1 mm cell was used. Directly before and after recording of CD spectra, absorbance spectra were measured with a Cary 14 or Cary

219 recording spectrophotometer to check that no absorbance changes had taken place during recording of CD spectra. Enzyme solutions were filtered with a Millipore filter of 0.45 μ pore size before use.

EPR spectra were recorded at 77°K with a Bruker model ER 420 X-band spectrometer. The field modulation amplitude was 5 G, the microwave frequency 9.210 GHz. Quartz sample tubes with a 3 mm inner diameter were used. Solutions of catalase were made up in 60% v/v glycerol buffer mixtures.

The molar ellipticity, $[\theta]_M$ in degrees·centimeters^2·decimoles^{-1} was calculated by the equation

$$[\theta]_M = 3300(\varepsilon_L - \varepsilon_R) \qquad (2)$$

where $(\varepsilon_L - \varepsilon_R)$ is the difference between the molar extinction coefficient for left and right circularly polarized light. Ellipticities below 250 nm were expressed as mean residue ellipticity $[\theta]_R = [\theta]_M/n$, where n, the number of residues per molecule, was taken to be 2020 (5). The equations of Chen et al. (18) were used to analyze the CD data between 210 and 243 nm for the distribution of α helical, β structure and random coil in the protein molecule.

2.4 Results

Spectra in Visible and Near-Ultraviolet Region

The CD and absorption spectra of native catalase and its cyanide and azide derivatives at pH 7.0 in the wave-

length range 250-700 nm are shown in Fig. 2.2. The absorption spectrum of native catalase exhibits three characteristic bands in the visible region at 505, 540 and 624 nm, the Soret band at 405 nm and the protein absorption band at 275 nm. The native enzyme shows negative CD bands at 388 and 640 nm and positive bands at 294, 420 and 550 nm. The addition of the ligand molecules cyanide and azide caused a complete loss of enzymatic activity as well as changes in the CD and absorption spectra. Cyanide binding to catalase caused a decrease in the intensity of the 388 and 640 peaks and new negative bands at 410 and 455 nm appeared. The intensity of the positive peak at 294 increased and a shoulder appeared at 340 nm. There was a decrease in the intensity of the band at 420 nm, a shift of the positive band to 530 nm and a new band at 590 nm. The absorption spectrum shows two bands in the visible region at 555 with a shoulder at 580-590 and a decrease and shift of the Soret band to 424 nm. The addition of azide caused a shift in the CD band at 388 nm and a new band at 330 nm appeared. The positive peak at 294 nm decreased, the 420 nm band increased and there was a shift of the peak at 550 nm to 530 nm. The absorption spectrum of the azide complex shows the characteristic three band spectra with different intensities than that of native enzyme. There is a new shoulder however at 580 nm which is not seen in native enzyme. The Soret band has shifted slightly with a small

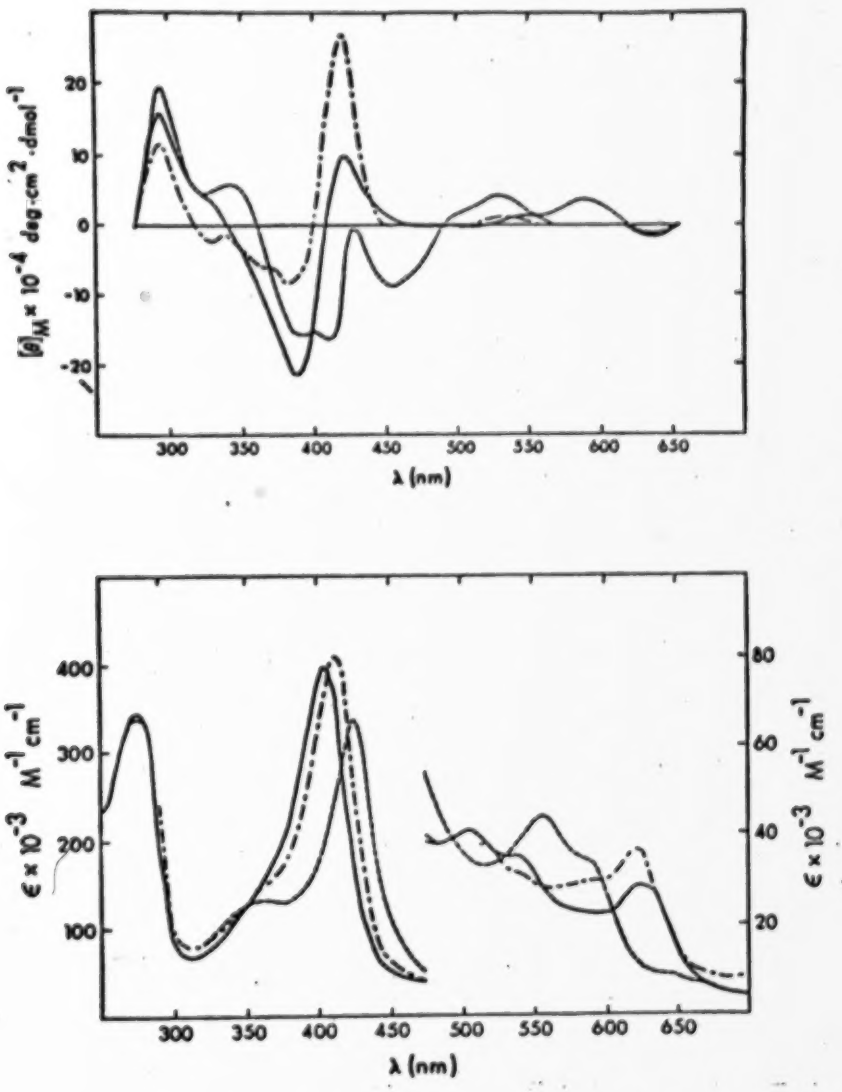

Fig. 2.2 Circular dichroism (upper) and absorption (lower) spectra of human erythrocyte catalase in the aromatic, Soret and visible regions. — native enzyme; --- cyanide complex; -·-· azide complex, all at pH 7.0 and 25°C.

increase in intensity. The results are outlined in Table 2.1. Fig. 2.3 shows the changes accompanying fluoride binding at pH 5.0. There is a shift of the 420 nm CD band to 415 nm and a decrease in the intensities of the other peaks. The binding of fluoride causes a loss of 40% of the enzyme activity, a decrease in the Soret absorption band and changes in the visible region (Table 2.1). Although the absorption spectrum of native enzyme is identical at pH 5.0 and 7.0, the CD spectrum shows a decrease in the band at 388 nm at lower pH values. The ligand molecules were removed by dialysis and the recovered solutions showed identical CD profiles to those of the native enzyme. The spectra of native enzyme remained unchanged from 9° to 54°C and over the pH range 5.7 to 9.6. Enzyme isolated from fresh and 21 day samples gave identical spectra.

Fig. 2.4 shows the effects of denaturation with acid at pH 2.9 and base at pH 12.0. There is a loss of all CD bands at wavelengths longer than 300 nm. The acid denaturation caused a blue-shift of the 294 band to 280 nm with a decrease in intensity whereas denaturation with alkali caused a shift to 250 nm with an enhancement of the band intensity. In the absorption spectrum (Fig. 2.5) alkaline treatment causes a shift of the 405 nm band to 390 nm with a decrease in intensity, a new peak at 360 nm and changes in the visible region. At pH 2.9 the Soret peak diminished and shifted to 380 nm and the intensities of visible bands decreased. On the other hand the absorp-

Table 2.1 Absorption and Circular Dichroic Spectra of Human Erythrocyte Catalase Complexes

Ligand	Absorption λ_{max}, nm	Absorption $\varepsilon \cdot 10^{-3}$ $M^{-1}cm^{-1}$	CD λ_{max}, nm	CD $[\theta]_M \cdot 10^{-4}$ $deg \cdot cm^2 \cdot dmol^{-1}$
Phosphate buffer pH 7.0	624	28.0	640	- 1.6
	540	35.2	550	1.2
	505	40.5	420	10.0
	405	397.0	388	-21.7
			294	16.1
Cyanide 0.1 mM pH 7.0	580-590(s)[a]	34.4	640	- 1.2
	555	44.9	590	3.8
	424	325.0	530	4.4
	360	119.0	455	- 8.4
			410	-16.1
			390	-15.3
			340	5.6
			294	19.2
Azide 100 mM pH 7.0	620	36.1	640	- 1.6
	580-590(s)	30.0	530	1.2
	540	31.2	420	26.9
	505	40.5	380	- 8.0
	413	411.0	330	- 2.0
			294	11.6
Fluoride 100 mM pH 5.0	600	43.8	550	1.0
	530	39.1	416	10.0
	485	47.4	385	-10.5
	405	365.0	298	8.1
Phosphate buffer pH 5.0	624	28.0	550	1.2
	540	35.2	420	10.0
	505	40.5	388	-17.3
	405	397.0	294	16.1

[a]Shoulder.

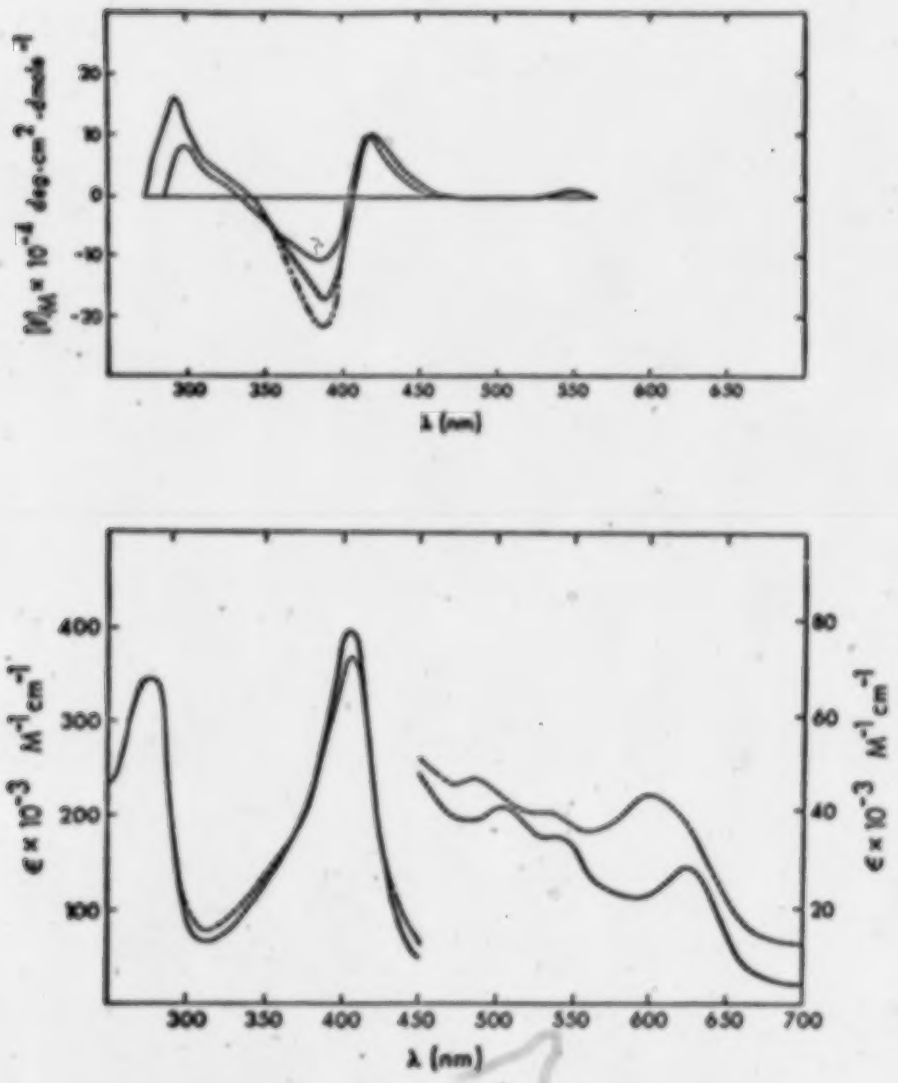

Fig. 2.3 Circular dichroism (upper) and absorption (lower) spectra of human erythrocyte catalase in the aromatic, Soret and visible regions. -·-· native enzyme pH 7.0; — native enzyme pH 5.0; --- fluoride complex pH 5.0.

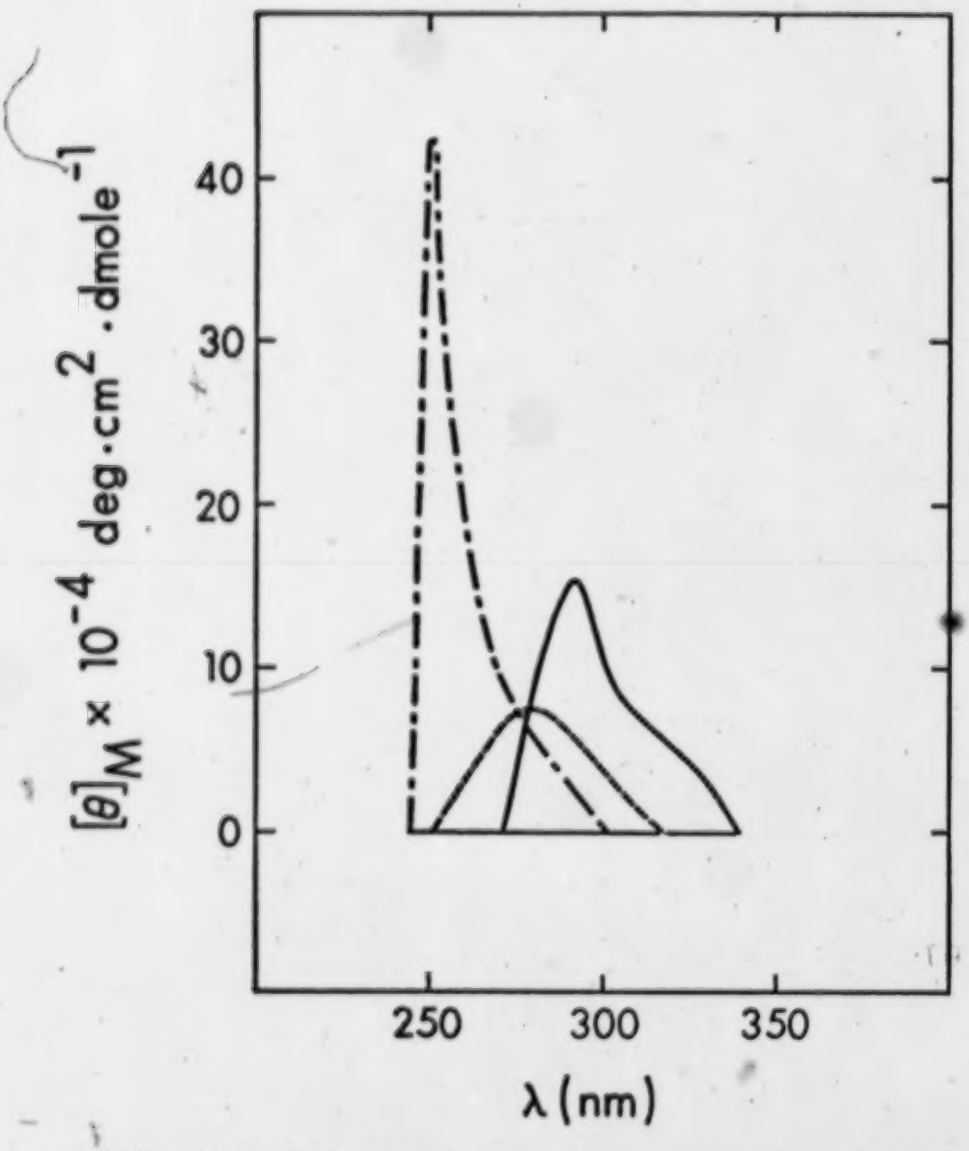

Fig. 2.4 Circular dichroism spectra of acid and alkaline treated catalase. — native enzyme pH 7.0; --- native enzyme pH 2.9; -·- native enzyme pH 12.0.

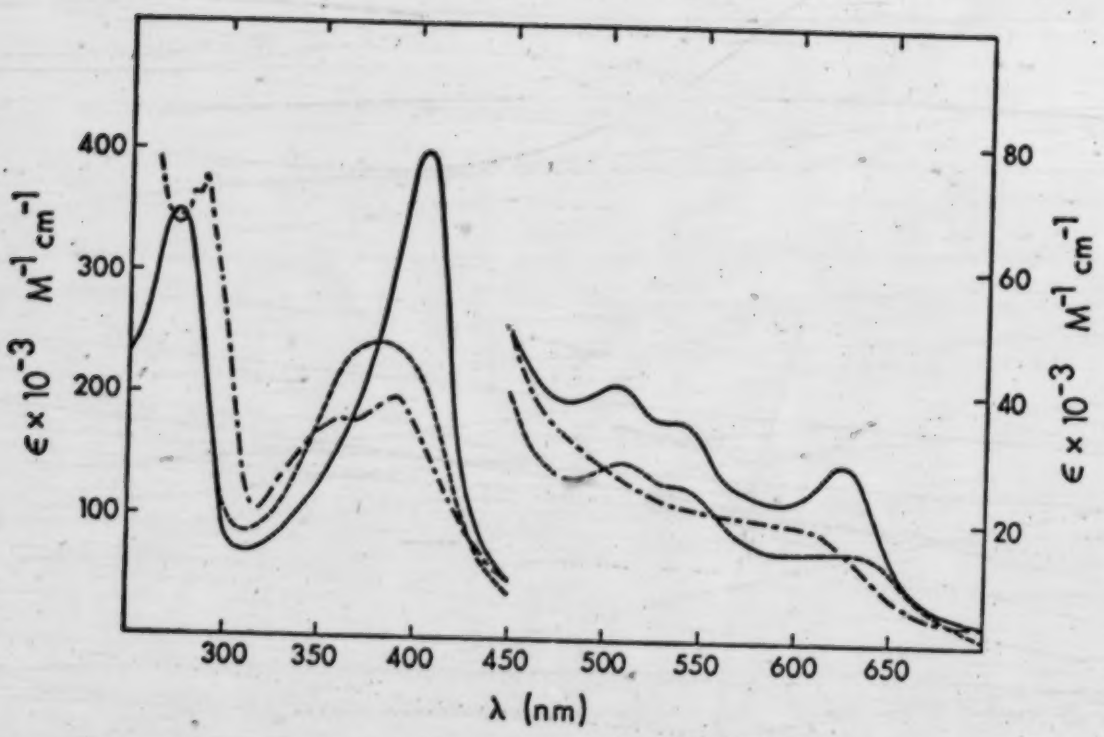

Fig. 2.5 Absorption spectra of acid and alkaline treated catalase. — native enzyme pH 7.0; --- native enzyme pH 2.9; -·-· native enzyme pH 12.0.

tion maximum at 275 nm remained virtually intact on acid denaturation.

Far Ultraviolet CD Spectra

In Fig. 2.6 the CD spectra of native, denatured and liganded catalase in the wavelength range 210-250 nm are illustrated. Average fractions of the secondary structure in human erythrocyte catalase calculated by the method of Chen et al. are 27% α helix, 9% β pleated sheet and 64% random coil. The theoretical curve predicted for these fractions is also shown in Fig. 2.6. The addition of the inhibitory ligand CN did not change the spectra. Acid and base caused the spectra to change dramatically with a complete loss of structure.

EPR Spectroscopy

Fig. 2.7 shows the EPR spectra of native human erythrocyte catalase and its cyanide derivatives. The free catalase spectrum has two intense signals g = 6.42 and 5.26 at low magnetic field, and a weak signal around g = 1.98 at high magnetic field. The cyanide complex shows three peaks with g values of 1.66, 2.24 and 2.84. Both show a weak signal at g = 2.00.

2.5 Discussion

The results in the far uv region indicate that the addition of cyanide to native catalase causes no detectable changes in the secondary structure of the protein. This has been shown for ligand binding to a number of

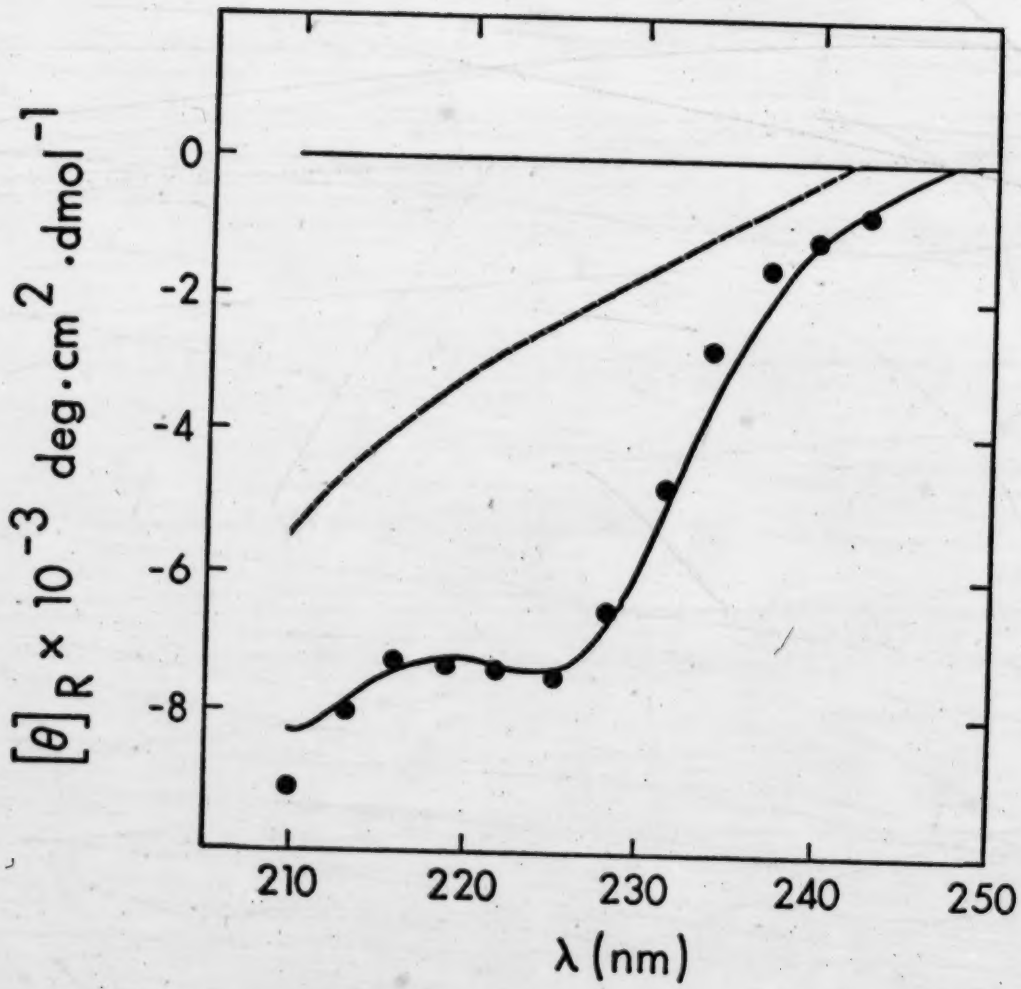

Fig. 2.6 Circular dichroism spectra in the far ultraviolet region. — native catalase pH 7.0 and cyanide complex; --- native catalase pH 2.9 and pH 12.0; ● ● ● calculated spectrum for 27% α helix, 9% β pleated sheet and 64% random coil configuration; the optical activities of the three conformations at any wavelength are those given by Chen et al. (18). The straight line at $[\theta]_R=0$ is the baseline.

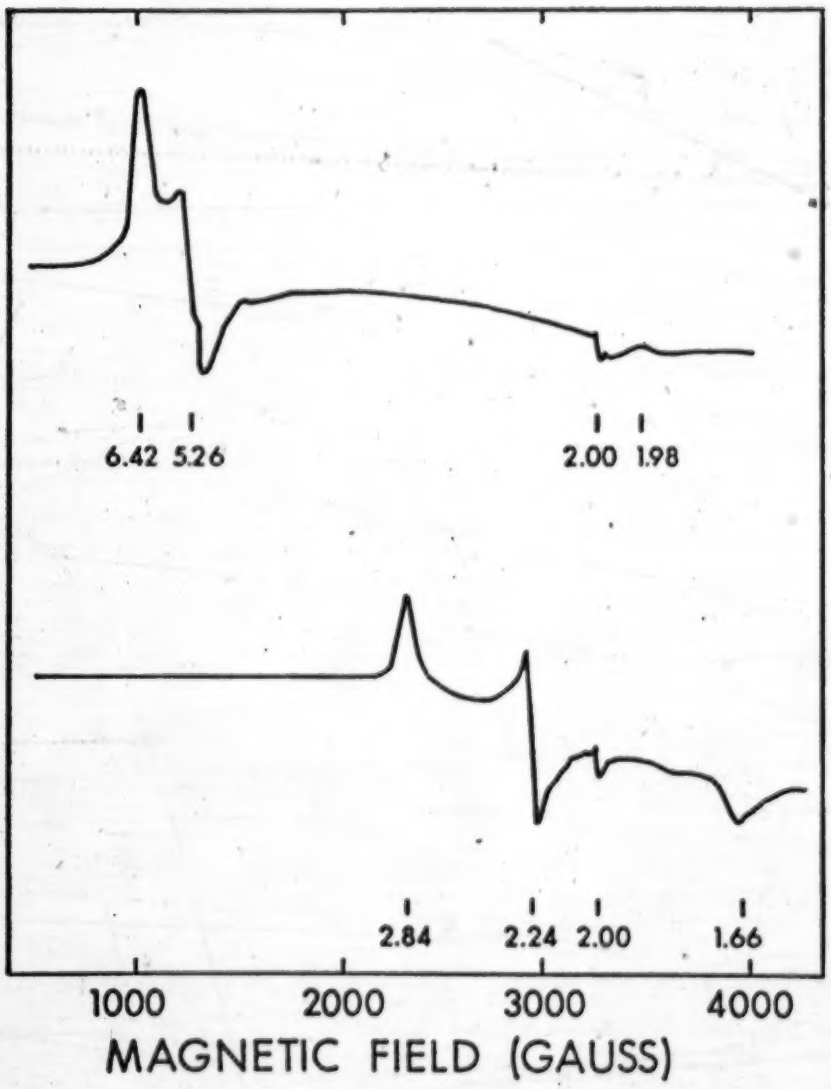

Fig. 2.7 First derivative of the EPR spectrum at 77°K of native human erythrocyte catalase (upper) and its cyanide derivative (lower) in 0.5 M phosphate buffer pH 7.0. Concentrations of enzyme and cyanide were 0.781 and 920 mM respectively. Microwave frequency was 9.210 G Hz.

hemoproteins including myoglobin (19,20); soybean leghemoglobin (21), horse erythrocyte catalase (22), Japanese radish and turnip peroxidase (23,24) and compound I and II formation for beef liver catalase (25). This is in contrast to the findings of Samejima and Kita (26) who reported a decrease in the helical content of beef liver catalase from 50% to 30% on the binding of cyanide or azide. The calculated content of α helical structure of human erythrocyte catalase is 27% which is comparable to the 35% and 29% calculated for horse and porcine erythrocyte enzymes respectively (22,27) and considerably lower than the 50% reported for native beef liver enzyme (26). Treatment with acid and alkali caused complete randomization of the molecule. The results are similar to the randomization seen after a urea treatment of *B. simplicifolia* lectin and cytochrome b_5 (28,29).

The changes in the CD spectra in the near ultraviolet and visible regions in the presence of acid and alkali are similar to those of Samejima and Kita (26) for beef liver catalase. The loss of CD bands above 300 nm may be due to denaturation in which the heme is still bound but no longer contributes to the optical activity or is detached from the protein (30). At pH 12.0 the CD band at 250 nm was found to be proportional to the number of ionized tyrosyl groups (31), and involves no significant contribution of protein.

The changes in the optical absorption spectra after acid or base treatment are also similar to those seen for other catalases and show spectra characteristic of acid and alkaline heme solutions (32,33). Basic treatment of beef liver or porcine erythrocyte enzyme produces a new peak at 362 nm, a decrease and shift of the Soret band maximum to 420 nm and an ultraviolet shift to 290 nm (34). The ultraviolet shift has been attributed to the exposure of embedded tyrosine residues and to ionization of tyrosine to the phenoxy form (35). The spectral changes for human erythrocyte enzyme are comparable but the Soret band shift is to 390 nm and not 420 nm as for the other enzymes. Jones et al. (36) have reported that for bacterial micrococcus enzyme, two overlapping peaks with maxima at about 355 and 392 nm replace the Soret band of native enzyme after alkaline treatment. They also related the degree of dissociation of the enzyme to the changes in the optical spectrum. The spectra of free heme in basic solutions also have both 360 and 390 nm peaks. Since alkaline treatment is known to dissociate native beef liver and bacterial catalase into four subunits of about 65,000 molecular weight (36-38), the alkaline treatment may result in both subunit formation and denaturation. The absorption spectral changes after acid treatment of human erythrocyte enzyme are a decrease in the intensity of the Soret band and a shift to 380 nm.

Beef liver enzyme shows identical changes (39) and the resulting spectra of both resemble that of free heme at pH 2.0 (33). Since acid treatment dissociates beef liver enzyme into 120,000 molecular weight subunits (39) the overall effect of acid treatment on human erythrocyte catalase may be splitting into heme and protein, and dissociation into subunits.

The absorption spectra of native enzyme in the visible and Soret regions show the group of bands typical of all metal porphyrins, B(γ), $Q_0(\alpha)$ and $Q_1(\beta)$ bands due to π-π^* transitions of the porphyrin ring and extra bands which are thought to arise from charge transfer transitions between the metal and the ring (40,41). For native erythrocyte catalase the bands at 624 and 505 nm are probably charge transfer bands, analogous to the charge transfer bands of beef liver, horse erythrocyte and bacterial micrococcus catalase at about 625 and 500 nm (41-43). These bands were found to be characteristic of a high spin ferric hemoprotein with five unpaired electrons. Similarly the band at 540 nm is the $Q_1(\beta)$ band. The absence or obscuring of the $Q_0(\alpha)$ band by charge transfer bands is further evidence for a high spin state (41,42).

The CD spectrum of native human erythrocyte enzyme from 250 to 700 nm resembles spectra reported for native porcine and horse erythrocyte catalases (27,43). They are quite different from that of beef liver enzyme (26).

This may be due to bile contaminant seen in liver but not blood catalases. The EPR spectra of liver enzymes show extra bands not seen for blood catalases and these have also been attributed to bile contaminants in the liver samples (6).

The absorption spectrum of the cyanide bound enzyme has distinct $Q_0(\alpha)$ and $Q_1(\beta)$ bands and the charge transfer bands are not evident. This is a characteristic of low spin compounds with one unpaired electron as is the shift of the Soret band to longer wavelengths after ligand binding (41).

The EPR spectrum of native enzyme shows three peaks g = 6.42, 5.26, 1.98 corresponding to rhombically distorted high spin ferric heme. This is in agreement with values reported by Williams-Smith and Patel (6) who find 3 peaks g = 6.50, 5.33 and 1.98 for human erythrocyte enzyme. The EPR signal at g = 2.00 is probably due to trace amounts of copper in the preparation. A similar signal was found for myeloperoxidase at g = 2.05 (44). All native catalases studied to data are in high spin state at neutral pH (6,43).

The EPR spectrum of the cyanide complex shows three signals with g values 2.84, 2.24 and 1.66 typical of a low spin ferric heme. These correspond to the signals with g values of 2.84, 2.25 and 1.66 found for the cyanide complex of horse erythrocyte and beef liver catalase (45,46).

EPR and magnetic susceptibility data (6,7,45,47) indicate that beef liver, bacterial, horse and human erythrocyte enzymes form a high spin complex on fluoride binding. The optical spectrum of human erythrocyte enzyme exhibits characteristics of a high spin complex and is similar to catalase isolated from other sources.

Azide complexes of catalase show a temperature dependence of the spin state. At room temperature magnetic susceptibility studies indicate the complex is of a high spin type but as the temperature is lowered to that of liquid nitrogen there is a mixture of high and low spin states (47,48). At room temperature the azide complex of erythrocyte enzyme has the spectral characteristics of a high spin compound, that is weak Q_0 and Q_1 bands and stronger charge transfer bands.

2.6 References

1. Bonnichsen, R.G. (1947) Arch. Biochem. 12, 83-94.
2. Herbert, D. and Pinsent, J. (1948) Biochem. J. 43, 203-205.
3. Stansell, M.J. and Deutsch, H.F. (1965) J. Biol. Chem. 240, 4299-4305.
4. Bonaventura, J., Schroeder, W.A. and Fang, S. (1972) Arch. Biochem. Biophys. 150, 606-617.
5. Aebi, H., Wyss, S.R., Scherz, B. and Skvaril, F. (1974) Eur. J. Biochem. 48, 137-145.

6. Williams-Smith, D.L. and Patel, K. (1975) Biochim. Biophys. Acta 405, 243-252.

7. Vuk-Pavlović, S. and Williams-Smith, D.L. (1977) Biochemistry 16, 5465-5470.

8. Greenfield, N. and Fasman, G.D. (1969) Biochemistry 8, 4108-4116.

9. Long, C., King, E.J. and Sperry, W.M. (1968) Biochemist's Handbook, pp. 1073 Spon, London.

10. Hartz, J.W. and Deutsch, H.F. (1972) J. Biol. Chem. 247, 7043-7050.

11. Green, A.A. and Hughes, W.L. (1955) Methods. Enzymol. 1, 67-90.

12. Jones, P. and Suggett, A. (1968) Biochem. J. 108, 833-838.

13. Hewson, W.D. and Dunford, H.B. (1976) J. Biol. Chem. 251, 6036-6042.

14. Shikama, K. and Yamazaki, I. (1961) Nature 190, 83-84.

15. Chervenka, C.H. (1969) A Manual of Methods for the Analytical Ultracentrifuge. Spinco Division of Beckman Instruments, Inc. Palo Alto, California.

16. Beers, R.F. and Sizer, I.W. (1952) J. Biol. Chem. 195, 133-140.

17. Porzio, M.A. and Pearson, A.M. (1977) Biochim. Biophys. Acta 490, 27-34.

18. Chen, Y.H., Yang, J.T. and Chow, K.H. (1974) Biochemistry 13, 3350-3359.

19. Breslow, E., Beychok, S., Hardman, K.D. and Gurd, F.R.N. (1965) J. Biol. Chem. 240, 304-309.

20. Samejima, T. and Yang, J.T. (1963) J. Mol. Biol. 8, 863-871.

21. Ellfolk, N. and Sievers, G. (1975) Biochim. Biophys. Acta 405, 213-227.

22. Jajczay, F.L., Ph.D. Thesis, University of Alberta (1970).

23. Hamaguchi, K., Ikeda, K., Yoshida, C. and Morita, Y. (1969) J. Biochem. (Tokyo) 66, 191-201.

24. Job, D. and Dunford, H.B. (1977) Can. J. Biochem. 55, 804-811.

25. Kajiyoshi, M. and Anan, F.K. (1977) J. Biochem. (Tokyo) 81, 1319-1325.

26. Samejima, T. and Kita, M. (1969) Biochim. Biophys. Acta 175, 24-30.

27. Takeda, A. and Samejima, T. (1977) J. Biochem. (Tokyo) 82, 1025-1033.

28. Lonngren, J., Goldstein, I.J. and Zand, R. (1976) Biochemistry 15, 436-440.

29. Huntley, T.E. and Strittmatter, P. (1972) J. Biol. Chem. 247, 4641-4647.

30. Urry, D.W. (1964) Proc. Natl. Acad. Sci. U.S.A. 54, 640-648.

31. Ikeda, K., Hamaguchi, K., Imanishi, M. and Amano, T. (1967) J. Biochem. (Tokyo) 62, 215-230.

32. Maehly, A.C. (1958) Acta Chem. Scand. 12, 1247-1258.

33. Maehly, A.C. (1952) Biochem. Biophys. Acta 8, 1-17.

34. Nagahisa, M. (1962) J. Biochem. (Tokyo) 51, 216-221.

35. Inada, Y. (1961) J. Biochem. (Tokyo) 49, 217-225.

36. Jones, P., Pain, R.H. and Suggett, A. (1970) Biochem. J. 118, 319-323.

37. Sund, H.W., Weber, K. and Mölbert, E. (1967) Eur. J. Biochem. 1, 400-410.

38. Samejima, T., McCabe, W.J. and Yang, J.T. (1968) Arch. Biochem. Biophys. 127, 354-360.

39. Samejima, T. and Yang, J.T. (1963) J. Biol. Chem. 238, 3256-3261.

40. Platt, J.R. (1956) in Radiation Biology (Hollaender, A., ed.) Vol. 3, pp. 71-123, McGraw-Hill Book Co., New York.

41. Brill, A.S. and Williams, R.J.P. (1961) Biochem. J. 78, 246-253.

42. Brill, A.S. and Sandberg, H.E. (1968) Biophys. J. 8, 669-690.

43. Yoshida, K., Iizuka, T. and Ogura, Y. (1970) J. Biochem. (Tokyo) 68, 849-857.

44. Bakkenist, A.R.J., Wever, R., Vulsma, T., Plat, H. and Van Gelder, B.F. (1978) Biochim. Biophys. Acta 524, 45-54.

45. Torii, K. and Ogura, Y. (1968) J. Biochem. (Tokyo) 64, 171-179.

46. Torii, K. and Ogura, V. (1969) J. Biochem. (Tokyo) 65, 825-827.

47. Deutsch, H.F. and Ehrenberg, A. (1952) Acta Chem. Scand. 6, 1522-1527.

48. Torii, K. and Ogura, Y. (1970) J. Biochem. (Tokyo) 68, 837-841.

2.7 Acknowledgments

I would like to thank the Canadian Red Cross and Dr. L.D. Wadsworth of the University of Alberta Hospital for providing blood samples. The disc gel electrophoresis was done by Mr. P. Nagainis. I also would like to thank Dr. C.M. Kay and Mr. M. Arabo for the ultracentrifugal work. Special thanks to Dr. A. Nadezhdin for the EPR spectroscopy and helpful discussions.

CHAPTER III.

THE REACTION OF HUMAN ERYTHROCYTE CATALASE WITH HYDROPEROXIDES TO FORM COMPOUND I

3.1 Summary

A kinetic study of the reaction of human erythrocyte catalase with peracetic acid, methyl hydroperoxide and ethyl hydroperoxide to form the primary oxidized compound (compound I) has been carried out at 25°C by means of a stopped flow technique. The pH dependence of the apparent second order rate constants indicates that the process occurs by reaction of catalase with unionized hydroperoxide molecules. The reaction of catalase with methyl hydroperoxide is pH independent in the range pH 5.8 to 9.4 and slows as methyl hydroperoxide (pK_a 11.5) is deprotonated. Similarly the reaction with peracetic acid is independent of pH from pH 5.8 to 6.5 and slows as peracetic acid (pK_a 8.2) is deprotonated.

The pH independent rate constants for the formation of compound I are 1.4×10^6, 2.7×10^4 and 3.8×10^4 $M^{-1}s^{-1}$ for methyl hydroperoxide, peracetic acid and ethyl hydroperoxide, respectively, following a trend of decreasing rate as the size of the substrate increases.

The optical absorption spectrum of compound I from 360 to 680 nm at pH 7.1 and 25°C obtained by a rapid scanning stopped flow technique is also reported.

3.2 Introduction

Catalase is a ferric hemoprotein which mediates the decomposition of hydrogen peroxide. In this catalatic reaction a molecule of hydrogen peroxide reacts with native enzyme to form a spectroscopically distinct intermediate, compound I, which reacts with a second molecule of hydrogen peroxide to give native enzyme, water and oxygen. It is difficult to study the formation of compound I with hydrogen peroxide because hydrogen peroxide reacts rapidly both as an oxidizing and reducing substrate for the enzyme and complete conversion to compound I is not possible.

Substituted peroxides can be used to examine the formation and properties of compound I since catalase reacts with an excess of these pseudo-substrates to form compound I which is stable for a few hundred milliseconds after the steady state is reached. Some aspects of compound I formation of catalase have been previously investigated. In a pioneering study Chance (1) showed that the rate of reaction of beef liver catalase with methyl hydroperoxide was independent of pH until the enzyme denatured. More recently Jones and Middlemiss (2) reported that beef liver and bacterial catalase react mainly with unionized peracetic acid molecules. Here compound I formation of human erythrocyte catalase is studied using a series of hydroperoxides. By using a pH jump technique to avoid enzyme denaturation the formation of compound I has been studied

over a wide pH range to determine whether the state of substrate protonation is always an important factor in the formation of compound I by catalase. In addition the optical absorption spectrum of compound I of human erythrocyte catalase was determined by a rapid scanning technique.

3.3 Experimental Procedures

Human erythrocyte catalase was isolated from 21-day-old blood samples as previously described (3). The enzyme was stored as a concentrate and passed through a Millipore filter of 0.45 μM pore size before use. The ratio of absorbances at 405 to 280 nm was used as an indication of purity and was greater than 1.2. The concentration of catalase was determined spectrophotometrically at 405 nm using a molar extinction coefficient of 3.97×10^5 M^{-1} cm^{-1} (4).

Methyl hydroperoxide was prepared as described by Criegee (5) but the first distillate was fractionally redistilled (25°, 15 torr). The hydrogen peroxide content of the first fractions was less than 4% as determined spectrophotometrically after the peroxide oxidation of iodide to iodine using molybdate as a catalyst (6). Total peroxide (methyl and hydrogen) was determined using horseradish peroxidase (Boehringer-Mannheim) as a catalyst (7). Peracetic acid was obtained from Pfaltz and Bauer Inc. as a 40% aqueous solution and was assayed iodometrically after pretreatment with catalase to remove hydrogen peroxide (2). Ethyl hydroperoxide was

purchased from Polysciences Inc. as a 10% aqueous solution, pretreated with catalase to remove any hydrogen peroxide and was assayed iodometrically (7). Potassium nitrate and all buffer components were reagent grade and used without further purification. Multidistilled water (8) was used in the preparation of all solutions.

Constant ionic strength buffers were prepared (9) and buffers were chosen to overlap whenever possible to test for specific buffer effects. In the pH range 5.8-6.2 citrate buffer was used, 5.9-8.7 phosphate buffer, 8.8-10.8 carbonate buffer, 10.7-11.9 phosphate buffer and 12.1-12.6 potassium hydroxide-potassium nitrate buffer. All solutions contained buffer contributing 0.05 to the total ionic strength of 0.11 with the remainder contributed by potassium nitrate. To test for the effect of nitrate, phosphate buffer contributing 0.10 to the total ionic strength and potassium nitrate contributing 0.01 were used in the peracetic acid study at pH 7.4 and 6.3.

Optical absorption spectra were measured with a Cary Model 219 spectrophotometer equipped with thermally jacketed cuvette holders.

All kinetic and rapid scan measurements were carried out on a Union Giken Model RA-601 stopped flow spectrophotometer equipped with a 1 cm cell thermostated to 25 ± 0.2°C. For a review of stopped flow methodology reference 10 should be consulted. The rapid scan absorption spectra are measured by means of a multi-channel photodiode with

a speed of 95 nm/ms and are memorized in a digital computer system. The analogue replica is afterwards obtained by use of a X-Y recorder. The dead time of the flow apparatus at the nitrogen gas pressure for the experiments was 1.5 ms. 95 nm regions were scanned from 360 to 680 nm with 10 nm overlap in all regions.

For kinetic measurements one reservoir of the stopped flow contained 0.2-0.5 μM catalase in 0.10 ionic strength buffer and the other at least a ten fold excess of hydroperoxide in 0.12 M potassium nitrate solution. At high pH values, greater than 11.4, a pH jump technique was used to avoid denaturation of catalase prior to mixing of the reaction solutions. Only the substrate contained buffer; the enzyme was in 0.12 M potassium nitrate solution. This method is feasible since the rate of compound I formation is faster than the rate of enzyme denaturation but slower than the rate of deprotonation of the enzyme when mixed with the buffer.

The reaction was followed at 404 nm in the absorbance mode, which resulted in a decrease in absorbance as a function of time. For the above conditions all kinetic curves were found to be first order. The observed rate constants were determined from a nonlinear least squares analysis (11). Six to ten determinations of the rate constant were performed; these were averaged for a single value with known standard deviation. The solutions were collected

after the reaction and their pH measured with a Fisher Model 420 pH meter in conjunction with a Fisher Micro Probe combination electrode calibrated with standard buffer solutions from Fisher.

3.4 Results

The spectral changes during the reaction of catalase with methyl hydroperoxide are shown in Fig. 3.1. The Soret peak of native catalase at 405 nm decreases to less than half the original intensity after compound I formation and is shifted to 399 nm. The distinct isobestic point at 435 nm indicates that compound I is the sole product of the reaction. Identical spectra were observed when 40 to 100 μM peracetic acid were used to form compound I, Fig. 3.2. Compound I formation is incomplete if ethyl hydroperoxide is used as a substrate. When 80 μM ethyl hydroperoxide was used as a substrate 45% of the enzyme was converted to compound I, for 350 μM or 1.4 mM ethyl hydroperoxide, 70% compound I was formed.

In the visible region from 450 to 680 nm, 300 μM methyl hydroperoxide was used to form compound I, Fig. 3.2. The isobestic points between native catalase and compound I are at 480 and 572 nm. The results are outlined in Table 3.1.

The concentration dependence of the kinetics of Compound I formation are shown in Figs. 3.3 and 3.4. No rate saturation was observed over the concentration range of

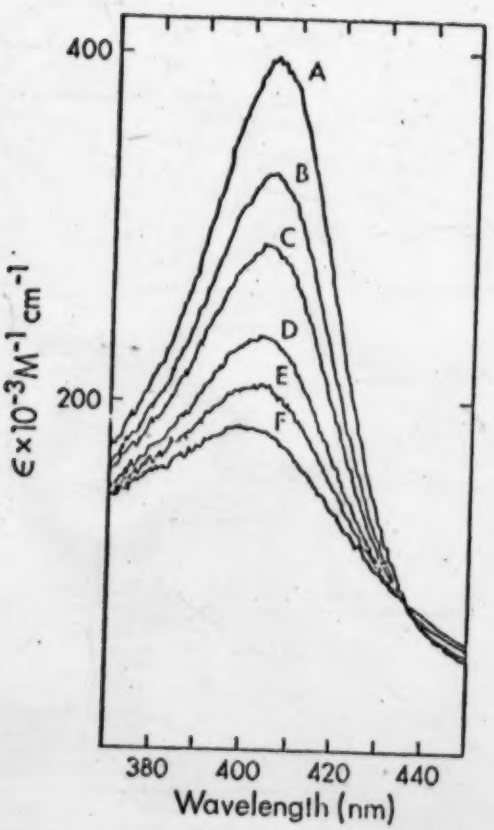

Fig. 3.1 Rapid-scan spectrophotometric measurement of the reaction of catalase with methyl hydroperoxide. All spectra obtained with 1 ms scanning times at pH 7.1 and 25°C. A, absorption spectrum of native catalase before reaction; B, the spectrum obtained during the dead time, identical to spectrum at stop of flow; C, spectrum scan started 2 ms after the stop of the flow; D, spectrum started 7 ms after the stop of the flow; E, 12 ms spectrum; F, 47 ms spectrum. Enzyme concentration 1.5 μM, methyl hydroperoxide concentration 100 μM.

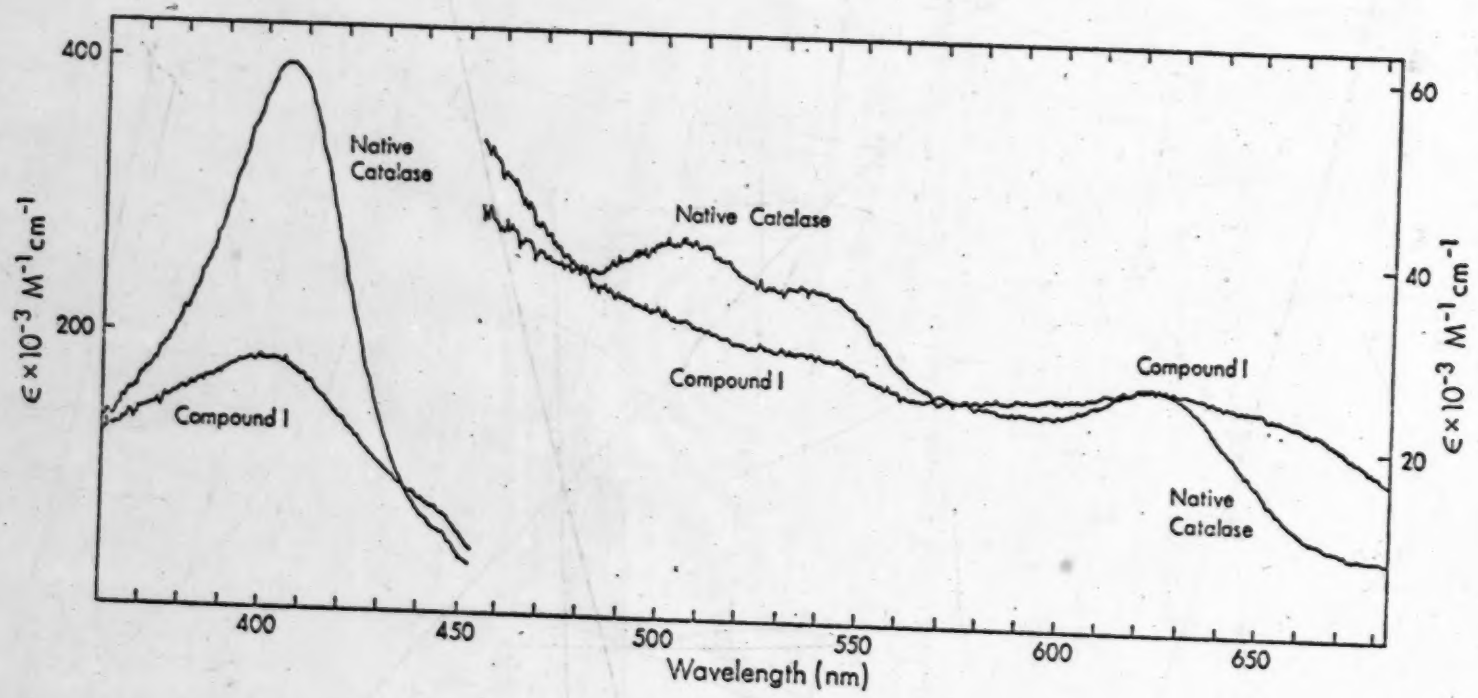

Fig. 3.2 Absorption spectra of native catalase and compound I in the Soret and visible regions. In the Soret region 80 μM peracetic acid and 1.5 μM catalase were used; in the visible region 300 μM methyl hydroperoxide and 9.8 μM catalase were used, all at pH 7.1 and 25°C.

Table 3.1 Wavelength maxima and extinction coefficients of optical spectra of human erythrocyte catalase and compound I.

Compound	Wavelength Maxima, nm	Extinction Coefficient $\varepsilon \times 10^{-3}$, $M^{-1}cm^{-1}$
Catalase pH 7.1, phosphate buffer 25°	405	397
	505	41
	540	35
	625	28
Compound I[a] pH 7.1, phosphate buffer 25°	399	180
	540[b]	29
	624	28

[a]Compound I formed by the addition of 40-100 μM methyl hydroperoxide or 80 μM peracetic acid to 1.5 μM catalase in Soret region or 300 μM methyl hydroperoxide to 9.8 μM catalase in the visible region.

[b]shoulder.

substrate which was used, 15 to 80 μM peracetic acid or 15 to 180 μM methyl hydroperoxide. At constant ionic strength at pH 6.3 and 7.4 the amount of nitrate had no effect on the observed rate constant. True second order kinetics are demonstrated by the linearity and zero intercept of each of these plots, obeying the following equation:

$$k_{obs} = k_{app}\ [\text{Hydroperoxide}] \qquad (1)$$

Values of k_{app} obtained in this manner are listed in Tables 3.2 and 3.3.

The apparent second-order rate constants, k_{app}, calculated from these results decreased markedly with increasing pH (Figs. 3.5, 3.6). Below pH 5.8 Compound I is not stable and decomposed before complete formation was achieved.

The simplest scheme which accounts for the k_{app} values is:

$$\begin{array}{l} E + SH \xrightarrow{k_1} \text{Compound I} \qquad (2) \\ \quad H^+ \uparrow\downarrow K_a \\ \quad\ S \end{array}$$

where K_a is the acid dissociation constant of the hydroperoxide and k_1 is the pH independent second-order rate constant for the reaction of enzyme and hydroperoxide.

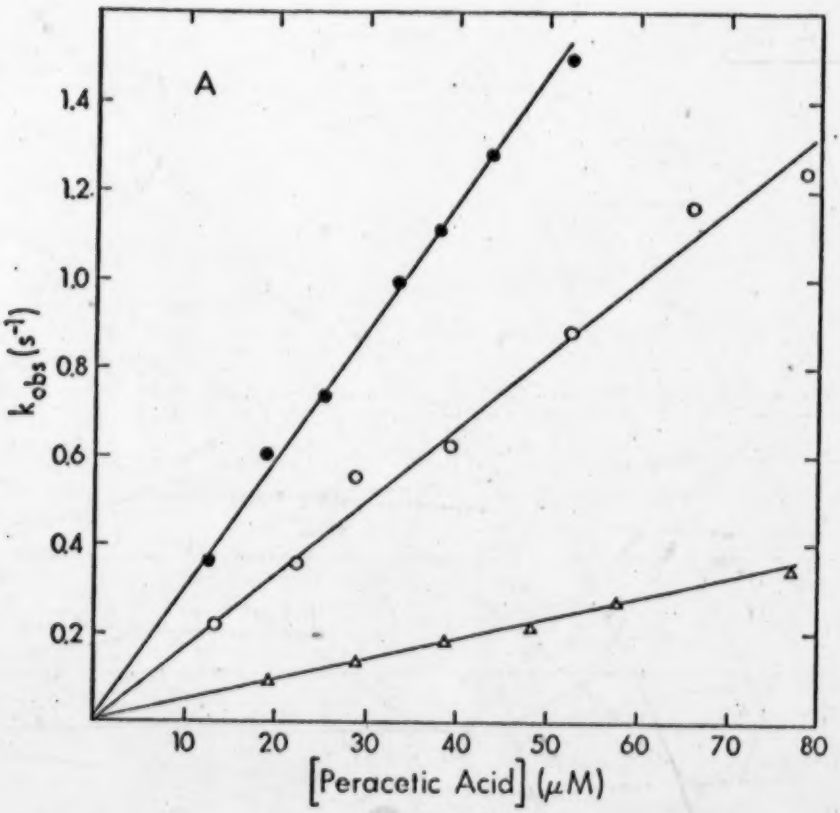

Fig. 3.3 Plots of k_{obs}, the pseudo first order rate constant for compound I formation vs. [Peracetic Acid]. Catalase concentration was 0.2 - 0.5 μM, temperature 25°C, total ionic strength 0.11. The slopes of the lines correspond to k_{app}, the second order rate constant and are calculated by a weighted linear least squares analysis. The intercepts are equal to zero within the standard deviation. ● pH = 6.61 phosphate buffer; ○ pH = 7.89 phosphate buffer; △ pH = 8.98 carbonate buffer.

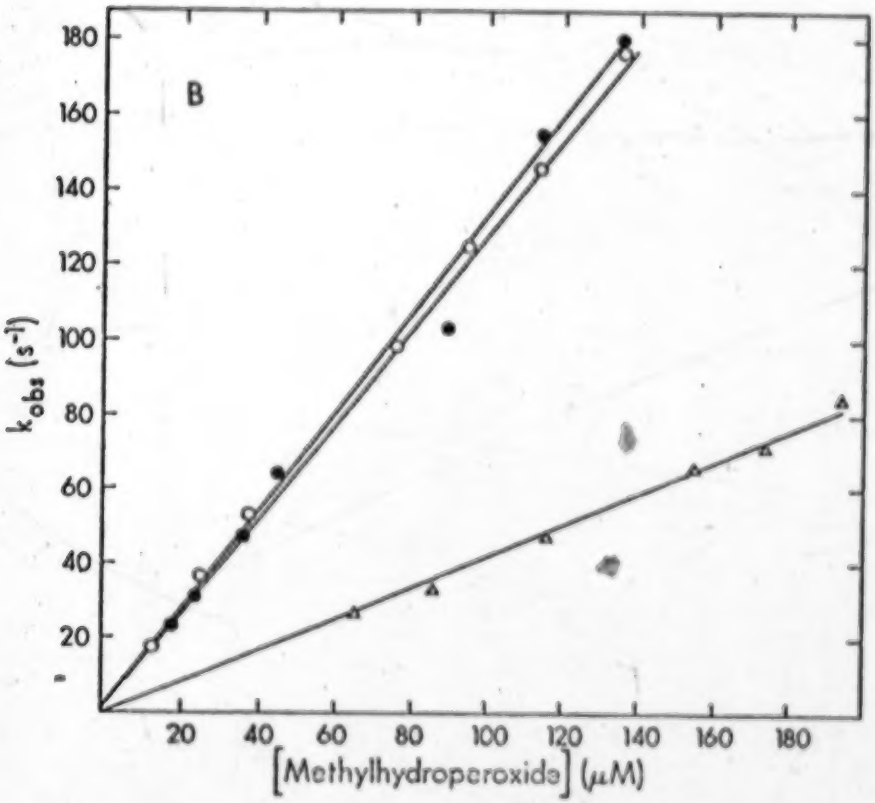

Fig. 3.4 Plots of k_{obs}, the pseudo first order rate constant for compound I formation vs. [methylhydroperoxide]. Catalase concentration was 0.2 - 0.5 μM, temperature 25°C, total ionic strength 0.11. The slopes of the lines correspond to k_{app}, the second order rate constant and are calculated by a weighted linear least squares analysis. The intercepts are equal to zero within the standard deviation. ○ pH = 5.85, phosphate buffer; ● pH = 9.17 carbonate buffer; △ pH = 11.59 phosphate buffer, pH jump technique.

Table 3.2 Rate Constants for the Formation of Compound I with Peracetic Acid[a]

pH	Buffer[b]	$k_{app} \times 10^{-4}$[c] ($M^{-1}s^{-1}$)
5.81	P	2.5 ± 0.1
6.12	P	3.0 ± 0.2
6.28	P	2.8 ± 0.1[d]
6.40	P	2.9 ± 0.2
6.61	P	2.84 ± 0.02[d]
6.85	P	2.41 ± 0.06[d]
7.13	P	2.8 ± 0.2
7.34	P	2.40 ± 0.06[d]
7.41	P	2.2 ± 0.1
7.43	P	2.3 ± 0.1
7.70	P	2.2 ± 0.1
7.75	P	2.02 ± 0.08
7.89	P	1.96 ± 0.08[d]
7.98	P	1.54 ± 0.08
8.27	P	1.3 ± 0.1
8.44	Ca	0.92 ± 0.07
8.56	Ca	0.82 ± 0.06
8.72	Ca	0.64 ± 0.03
8.75	Ca	0.66 ± 0.02
8.82	Ca	0.57 ± 0.04
8.95	Ca	0.38 ± 0.03
9.10	Ca	0.32 ± 0.04
9.15	Ca	0.19 ± 0.01
9.28	Ca	0.250 ± 0.009
9.47	Ca	0.149 ± 0.009
8.98	Ca	0.44 ± 0.02[d]
9.57	Ca	0.103 ± 0.007
9.67	Ca	0.103 ± 0.009
9.85	Ca	0.083 ± 0.004
9.69	Ca	0.069 ± 0.005
10.08	Ca	0.045 ± 0.001

Table 3.2 continued.

[a]Measurements carried out at 25°, ionic strength 0.11.

[b]Buffer code: P, KH_2PO_4-NaOH; Ca, $NaHCO_3$-NaOH.

[c]k_{app} determined by dividing the pseudo-first order rate constant by the appropriate peracetic acid concentration, unless otherwise indicated. Error is the standard deviation of the mean value of k_{app}.

[d]k_{app} determined from the slope of k_{obs} versus [peracetic acid]. Error is the standard deviation calculated by the least squares analysis.

Table 3.3 Rate Constants for the Formation of Compound I with Methyl Hydroperoxide[a]

pH	Buffer[b]	$k_{app} \times 10^{-6}$ [c] ($M^{-1}s^{-1}$)
5.81	Ci	1.50 ± 0.06
5.85	P	1.21 ± 0.02[d]
6.04	P	1.35 ± 0.06
6.23	P	1.34 ± 0.05
6.23	Ci	1.51 ± 0.05
6.43	P	1.36 ± 0.04
6.62	P	1.35 ± 0.04
6.66	P	1.39 ± 0.06
6.82	P	1.23 ± 0.04
6.83	P	1.38 ± 0.04
7.08	P	1.25 ± 0.06[d]
7.22	P	1.33 ± 0.04
7.45	P	1.38 ± 0.08
7.68	P	1.38 ± 0.03
8.00	P	1.37 ± 0.03
8.36	P	1.44 ± 0.08
8.69	P	1.43 ± 0.05
8.84	Ca	1.40 ± 0.03
9.17	Ca	1.31 ± 0.03[d]
9.28	Ca	1.43 ± 0.01
9.31	Ca	1.44 ± 0.04
9.44	Ca	1.32 ± 0.02
9.88	Ca	1.37 ± 0.06
10.36	Ca	1.18 ± 0.02
10.63	Ca	1.13 ± 0.03
10.68	P	1.04 ± 0.03
10.82	Ca	1.02 ± 0.03
10.84	Ca	0.99 ± 0.03
10.96	Ph	0.89 ± 0.04
11.20	Ph	0.73 ± 0.08
11.43	Ph	0.60 ± 0.02[e]
11.48	Ph	0.38 ± 0.02[e]
11.59	Ph	0.44 ± 0.01[d]
11.60	Ph	0.426 ± 0.004
11.90	Ph	0.216 ± 0.004
12.12	K	0.18 ± 0.01
12.24	K	0.27 ± 0.02
12.52	K	0.13 ± 0.02
12.60	K	0.073 ± 0.005

Table 3.3 continued.

[a]Measurements carried out at 25°, ionic strength 0.11.

[b]Buffer code: Ci, citric acid-sodium citrate; P, KH_2PO_4-NaOH; Ca, $NaHCO_3$-NaOH; Ph, Na_2HPO_4-NaOH; K, KOH-KNO_3.

[c]k_{app} determined by dividing the pseudo-first order rate constant by the appropriate methyl hydroperoxide concentration, unless otherwise indicated. Error is the standard deviation of the mean value of k_{app}.

[d]k_{app} determined from the slope of k_{obs} versus [methyl hydroperoxide]. Error is the standard deviation calculated by the least squares analysis.

[e]Measurement at pH 11.48 carried out by means of pH jump technique; measurement at pH 11.43 carried out with enzyme pre-equilibrated to the pH of measurement to verify overlap of pH jump and other measurements.

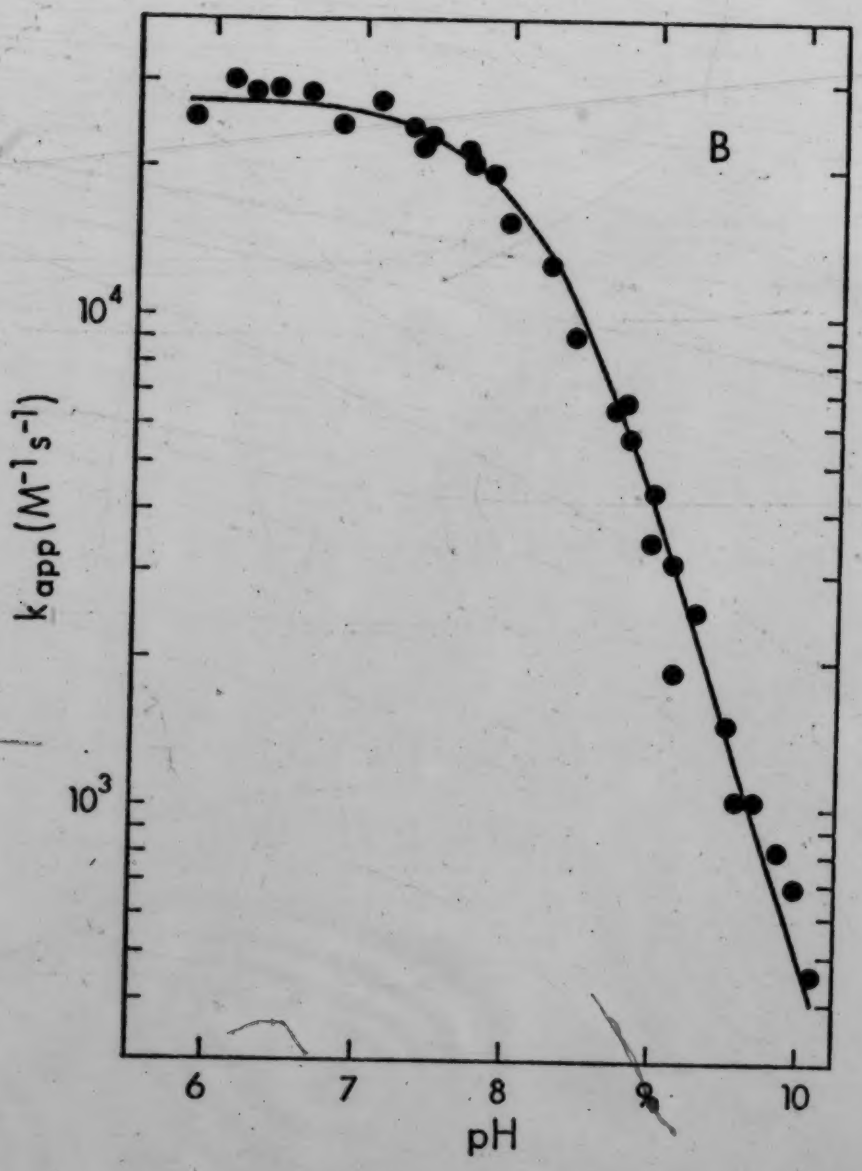

Fig. 3.5 The pH dependence of compound I formation with peracetic acid. The best line through the data was calculated using a nonlinear least squares analysis of Equation 3.

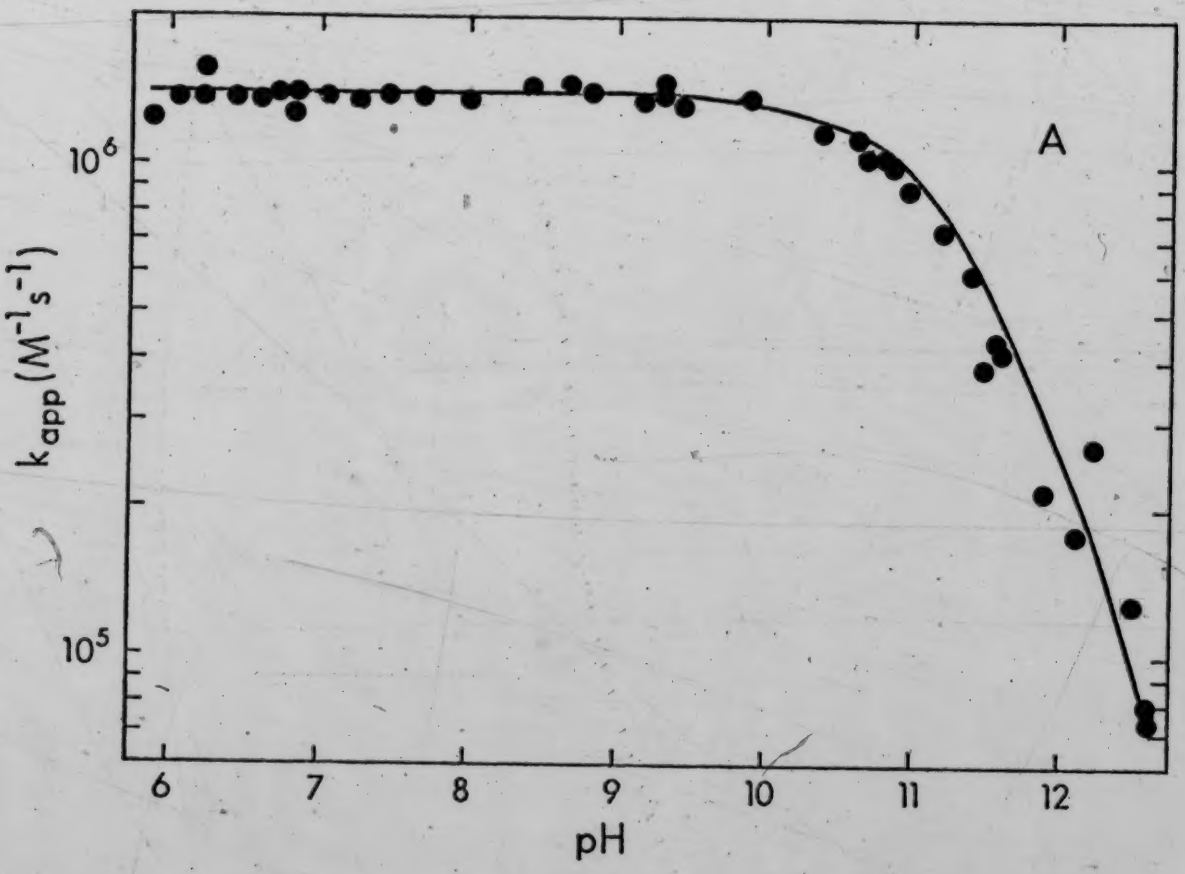

Fig. 3.6 The pH dependence of compound I formation with methyl hydroperoxide. The best line through the data was calculated using a nonlinear least analysis of Equation 3.

The apparent second-order rate constant, k_{app} is given by:

$$k_{app} = \frac{k_1}{1 + \frac{K_a}{[H^+]}} \qquad (3)$$

Analysis of the k_{app} vs. pH rate profiles using a nonlinear least squares analysis program (12) give values of pK_a and k_1 compiled in Table 3.4.

Ethyl hydroperoxide, pK_a 11.8 (13) was studied in the pH independent region 6.30 to 9.23. No rate saturation was observed in the order plot at pH 7.0 for 41 μM to 4.3 μM ethyl hydroperoxide (Fig. 3.7). The pseudo-first order rate constants were also directly proportional to ethyl hydroperoxide concentration. The value of k_{app} which equals k_1 is $(3.8 \pm 0.2) \times 10^4\ M^{-1}s^{-1}$.

3.5 Discussion

When hydroperoxides react with catalase an intermediate, compound I is formed. As compound I disappears compound II and native catalase appear. The formation of compound I is a bimolecular reaction between catalase and hydroperoxide following second order kinetics over a wide range of hydroperoxide concentrations. It is a 2 electron oxidation of native enzyme to form a formal Fe(V) species (14). The reaction is very complex and is essentially irreversible. It has been shown that oxygen is retained

Table 3.4 Compound I formation. Kinetic parameters obtained by a non-linear least squares analysis of the data in Fig. 3 according to Equation 3.

Parameter[a]	Methyl Hydroperoxide	Peracetic Acid
k_1 ($M^{-1}s^{-1}$)	$(1.40 \pm 0.04) \times 10^6$	$(2.7 \pm 0.1) \times 10^4$
pK_a	11.37 ± 0.04	8.25 ± 0.03
pK_a' [b]	11.5 ± 0.2 (13)	8.2 (28)

[a]Errors are standard deviations by the nonlinear least squares analyses.

[b]Literature values of pK_a's of methyl hydroperoxide and peracetic acid.

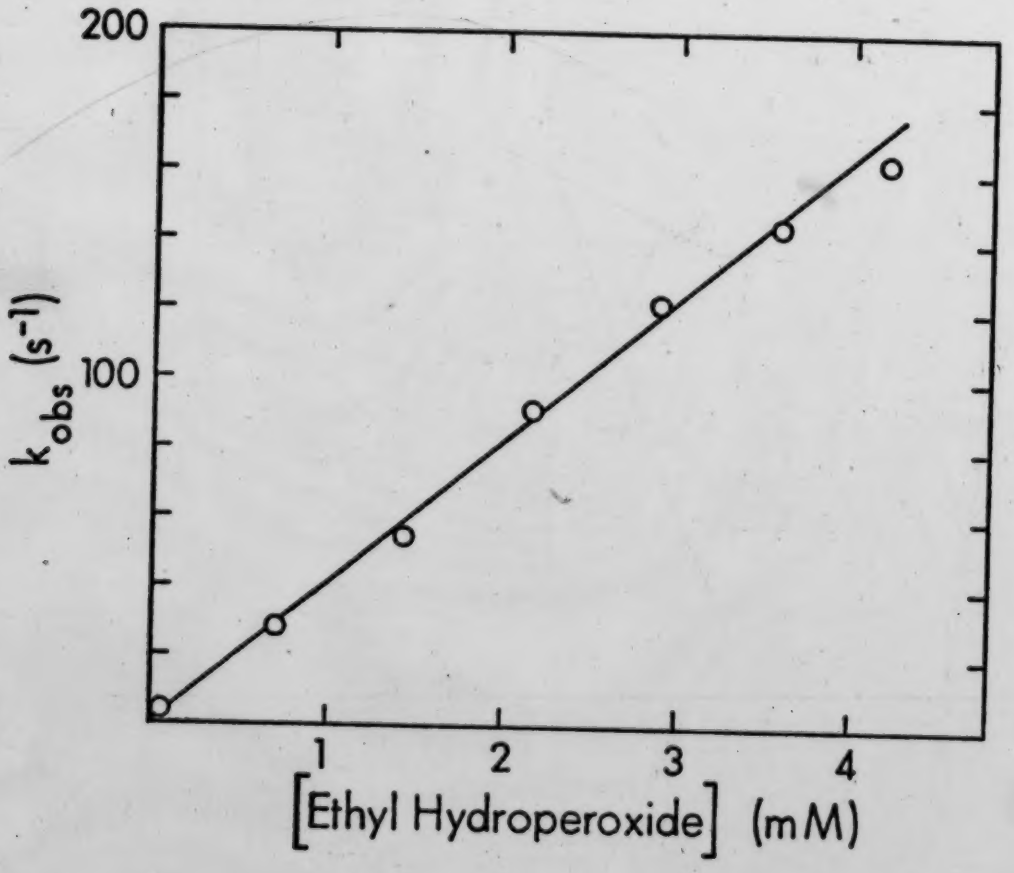

Fig. 3.7 Plot of k_{obs}, the pseudo first order rate constant for compound I formation vs. [ethyl hydroperoxide]. Catalase concentration 0.3 μM; temperature 25°; total ionic strength 0.11; pH 7.0, phosphate buffer. Slopes of the lines correspond to k_{app} the second order rate constant and are calculated by a weighted linear least squares analysis.

in chloroperoxidase compound I (15), and horseradish peroxidase compound I (16). It is generally supposed that retention of an oxygen atom is a general feature of compound I formation reactions of catalase and peroxidases (17).

In order to ensure complete formation of catalase compound I an excess of hydroperoxide must be used. This resembles the behaviour of myeloperoxidase[1] and is unlike the vegetable peroxidases that form compound I completely after the addition of an equivalent of peroxide. The compound I spectrum is independent of the oxidant used in its preparation.

The spectra obtained for erythrocyte compound I differ from spectra reported previously. Although the extinction coefficient of 1.8×10^5 $M^{-1}cm^{-1}$ at 398 nm agrees with values for horse erythrocyte (18) and microbial (14) catalase the visible region does not show the distinct band at 660 nm reported in these titration determinations.

Arguments have been made on the basis of the peak at 660 nm that catalase compound I is an Fe(IV) porphyrin π-cation radical with a $^2A_{1u}$ ground state (19). It is difficult to assign the ground state for human erythrocyte catalase but the possibility remains that compound I is a

[1] Harrison, J.E., Araiso, T., Palcic, M.M. and Dunford, H.B. (1980) Biochem. Biophys. Res. Commun.

π-cation radical. In cytochrome *c* peroxidase the free radical of compound I is probably located on an amino acid residue (20) and it has been suggested that the radical of horseradish peroxidase compound I is near the paramagnetic center on an amino acid residue (17,21,22).

The formation of compound I has been shown to be by reaction of erythrocyte catalase with unionized peracetic acid and methyl hydroperoxide molecules. Bacterial enzyme reacts similarly with peracetic acid whereas beef liver enzyme appears to react at least partly with ionized peracetic acid molecules (2). In addition the size of the substrate provides a constraint on the reaction with the rate of reaction decreasing as the size of the alkyl group of the substrate increases. The rate constants for the formation of compound I with peracetic acid and ethyl hydroperoxide are comparable, in agreement with the idea that the size of the end group restricts access to the active site of catalase.

No kinetically important ionizations on the enzyme have been detected although a recent EPR study on native beef liver enzyme suggests a group with a pK_a of 6.0 influences the rhombic environment of the heme (23). This may be related to the instability of compound I below pH 5.8 and the change in the CD and MCD spectra of native enzyme below pH 5 (24,25).

The stoichiometry of the reaction has been studied with peracetic acid and bacterial catalase and it was found that one mole of acetic acid is released per mole of catalase heme converted to compound I (26). Ethyl hydroperoxide is converted mainly to acetaldehyde (27) while some ethanol is formed (18). The product of the reaction with methyl hydroperoxide is 85% methanol and the low yield of formaldehyde may be attributed to a rapid diffusion of methanol from the active site (21). Conversely, the high conversion of ethyl hydroperoxide to acetaldehyde could result from a slower diffusion of ethanol from the active site, allowing compound I to react with ethanol.

The reactivity of erythrocyte enzyme is higher than beef liver enzyme presumably since erythrocyte catalase contains four intact heme groups whereas beef liver catalase has some degraded to bile pigments. Both erythrocyte and liver enzymes have far greater reactivity than microbial enzyme (2) which has four intact heme groups. The reason for the decreased reactivity of microbial enzyme is unclear but is possibly due to different amino acid residues in the active site. Indeed it is the protein around the heme group that accounts for the diversity of biochemical functions of heme containing molecules. These include oxygen transport and storage by hemoglobin and myoglobin, electron transport by cytochromes and peroxidatic and catalatic decompositions mediated by peroxidases and catalase.

3.6 References

1. Chance, B. (1952) J. Biol. Chem. 194, 471-481.
2. Jones, P. and Middlemiss, D.N. (1972) Biochem. J. 130, 411-415.
3. Aebi, H., Wyss, S.R., Scherz, B. and Skvaril, F. (1974) Eur. J. Biochem. 48, 137-145.
4. Bonaventura, J., Schroeder, W.A. and Fang, S. (1972) Arch. Biochem. Biophys. 150, 606-617.
5. Criegee, R. (1952) in Houben-Weyl, Methoden der Organischen Chemie, 4th ed. 8, (Muller, E., ed.) pp. 34-35, Thieme, Stuttgart.
6. Ovenston, T.C.J. and Rees, W.T. (1950) Analyst (London) 75, 204-208.
7. Cotton, M.L. and Dunford, H.B. (1973) Can. J. Chem. 51, 582-587.
8. Hewson, W.D. and Dunford, H.B. (1976) J. Biol. Chem. 251, 6036-6042.
9. Bates, R.G. and Bowen, V.E. (1956) Anal. Chem. 28, 1322-1324.
10. Gibson, Q.H. (1969) Methods in Enzymology 16, 187-228.
11. Roman, R., Dunford, H.B. and Evett, M. (1971) Can. J. Chem. 49, 3059-3063.
12. Hasinoff, B.B. and Dunford, H.B. (1970) Biochemistry 9, 4930-4939.

13. Everett, J. and Minkoff, G.J. (1953) Trans. Far. Soc. 49, 410-415.

14. Brill, A.S. and Williams, R.J.P. (1961) Biochem. J. 78, 253-262.

15. Hager, L.P., Doubek, D.L., Silverstein, R.M., Hargis, J.H. and Martin, J.C. (1972) J. Am. Chem. Soc. 94, 4364-4366.

16. Schonbaum, G.R. and Lo, S. (1972) J. Biol. Chem. 247, 3353-3360.

17. Jones, P. and Dunford, H.B. (1977) J. Theor. Biol. 69, 457-470.

18. Schonbaum, G.R. and Chance, B. (1976) in The Enzymes Vol. XIII Part C. (Boyer, P.D., ed.) pp. 363-408, Academic Press, New York.

19. DiNello, R.K. and Dolphin, D. (1979) Biochem. Biophys. Res. Commun. 86, 190-198.

20. Yonetani, T., Schleyer, H. and Ehrenberg, A. (1966) J. Biol. Chem. 241, 3240-3243.

21. Aasa, R., Vänngård, T. and Dunford, H.B. (1975) Biochim. Biophys. Acta 391, 259-264.

22. Schulz, C.E., Devaney, P.W., Winkler, H., Debrunner, P.G., Doan, N., Chiang, R., Rutter, R. and Hager, L.P. (1979) FEBS Lett. 103, 102-105.

23. Blum, H., Chance, B. and Litchfield, W.J. (1978) Biochim. Biophys. Acta 534, 317-321.

24. Palcic, M. and Dunford, H.B. (1979) Can. J. Biochem. 57, 321-329.

25. Brewett, W.R. and Stillman, M.J. (1979) Biochim. Biophys. Acta 577, 291-306.

26. Jones, P. and Middlemiss, D.N. (1974) Biochem. J. 143, 473-474.

27. Stern, K.G. (1936) J. Biol. Chem. 114, 473-494.

28. Koubek, E., Haggett, M.L., Battaglia, C.J., Ibne-Rasa, K.M., Pyun, H.Y. and Edwards, J.O. (1963) J. Amer. Chem. Soc. 85, 2263-2268.

3.7 Acknowledgments

I would like to thank the Canadian Red Cross for providing us with blood samples and Mr. O. Hindsgaul for the synthesis of methyl hydroperoxide.

3.8 Appendix

The following is the derivation of Equation 3.

$$v = k_{app}[E]_{total}[S]_{total} = k_1[E][SH]$$

$$[E]_{total} = [E]$$

$$[S]_{total} = [SH] + [S]$$

$$k_{app} = \frac{k_1[E][SH]}{[E]\ ([SH] + [S])}$$

$$k_{app} = \frac{k_1}{1 + \frac{K_a}{[H^+]}}$$

CHAPTER IV.

THE KINETICS OF CYANIDE BINDING BY HUMAN ERYTHROCYTE CATALASE

4.1 Summary

The kinetics of the binding reaction of cyanide by human erythrocyte catalase at 25° have been studied over the pH range 4.2 to 10.2 by means of temperature jump and stopped flow techniques. Catalase reacts with cyanide at a constant rate in the range pH 4.2 to 8.1 which decreases at higher pH. This is most simply explained by the reaction of catalase with unionized hydrogen cyanide molecules. The pH independent rate constant for the formation of the catalase-cyanide complex is $(1.3 \pm 0.1) \times 10^6$ $M^{-1}s^{-1}$. The association equilibrium constant and the dissociation rate constant for the catalase-cyanide complex were determined by spectrophotometric titration and from the relaxation amplitudes of temperature jump experiments and are $(3.1 \pm 0.2) \times 10^5$ M^{-1} and 4.2 ± 0.6 s^{-1} respectively in the pH independent region.

4.2 Introduction

Human erythrocyte catalase is a ferric hemoprotein which mediates the decomposition of hydrogen peroxide. It was shown in Chapter III (1), that the enzyme reacts with the protonated form of a variety of peroxides, but the reaction could not be studied below pH 5.8, since the intermediate

compound I formed in the reaction is unstable and decomposed before complete formation was achieved. Here the pH range has been extended by using cyanide as a probe of the active site of erythrocyte catalase. In an earlier study (2) the effect of pH on the dissociation constant of the catalase cyanide complex was reported. The dissociation constant followed the theoretical curve for the dissociation of hydrocyanic acid but there were unexplained deviations. By using temperature jump, stopped flow and spectroscopic techniques a detailed study of the effect of pH on the forward and reverse rate constants and the association constant of cyanide binding to human erythrocyte catalase was carried out.

4.3 Experimental Procedures

Human erythrocyte catalase with a 405/275 absorbancy ratio greater than 1.2 was isolated from 21-day-old blood samples as described in Chapter II. The concentration of catalase was determined spectrophotometrically at 405 nm using a molar absorptivity of 3.97×10^5 M^{-1} cm^{-1} (4). Triply distilled water was used to prepare all solutions. Inorganic chemicals of reagent grade were used without further purification. Fresh potassium cyanide stock solutions were standardized before or after use by titration with standard silver nitrate solution (5). Buffers of ionic strength 0.11 were used for all determinations (6).

A Fisher Model 420 pH meter in conjunction with a Fisher Micro Probe combination electrode was used for pH measurements and a Cary Model 219 spectrophotometer equipped with thermally jacketed cuvettes was used for absorption measurements. All stopped flow and temperature jump measurements were carried out on a Union Giken Model RA-601 Rapid Reaction Analyzer. For temperature jump experiments, the discharge from a 0.2 μF capacitor charged to 8 kV was used to cause a temperature change of about 2.8° as determined by measuring the temperature-induced absorption change for a solution of phenol red. The reaction cell was maintained at 22.2° so that the temperature of the kinetic experiments was approximately 25°. The volume and optical path length of the sample cell were 1.2 ml and 0.94 cm. Relaxation times for the binding of cyanide to human erythrocyte catalase were determined by adding small volumes of concentrated cyanide solution to a buffered solution of enzyme, then placing immediately the mixed solution into the temperature jump cell; thus, the loss of cyanide at low pH values was minimized. The reaction was followed at 402 nm where an increase of absorbance as a function of time was observed. For all reactions studied a single relaxation was observed. At each cyanide concentration six to eight determinations of the relaxation time and amplitude were performed; these were averaged for a single value. The relaxation time was determined by a

non-linear least squares analysis of the first order curve (7). The relaxation amplitude was measured on an X-Y recorder.

For stopped flow measurements one reservoir of the stopped flow contained 0.2 - 0.5 μM catalase in 0.22 ionic strength buffer and the other at least a ten fold excess of cyanide in aqueous solution. The association reaction was followed at 404 nm in the absorbance mode, where a decrease in absorbance as a function of time occurred. For the above conditions all kinetic curves were found to be first order and the observed rate constants were also determined from a non-linear least squares analysis.

4.4 Results

The optical spectrum of human erythrocyte catalase and its cyanide complex has been reported previously (3). The addition of cyanide to catalase causes changes in the optical spectrum of the heme groups, a decrease in the extinction and shift in the maximum of the Soret peak to longer wavelengths. Here the difference in absorbance with increasing concentrations of cyanide is used to determine the association constant K_{CN} for cyanide binding by means of a Scatchard plot (8) (Fig. 4.1). The number of binding sites per heme of catalase is approximately one in all cases. The values of the equilibrium constant determined from the slope and the intercept of Scatchard plots decreased as pH increases (Table 4.1).

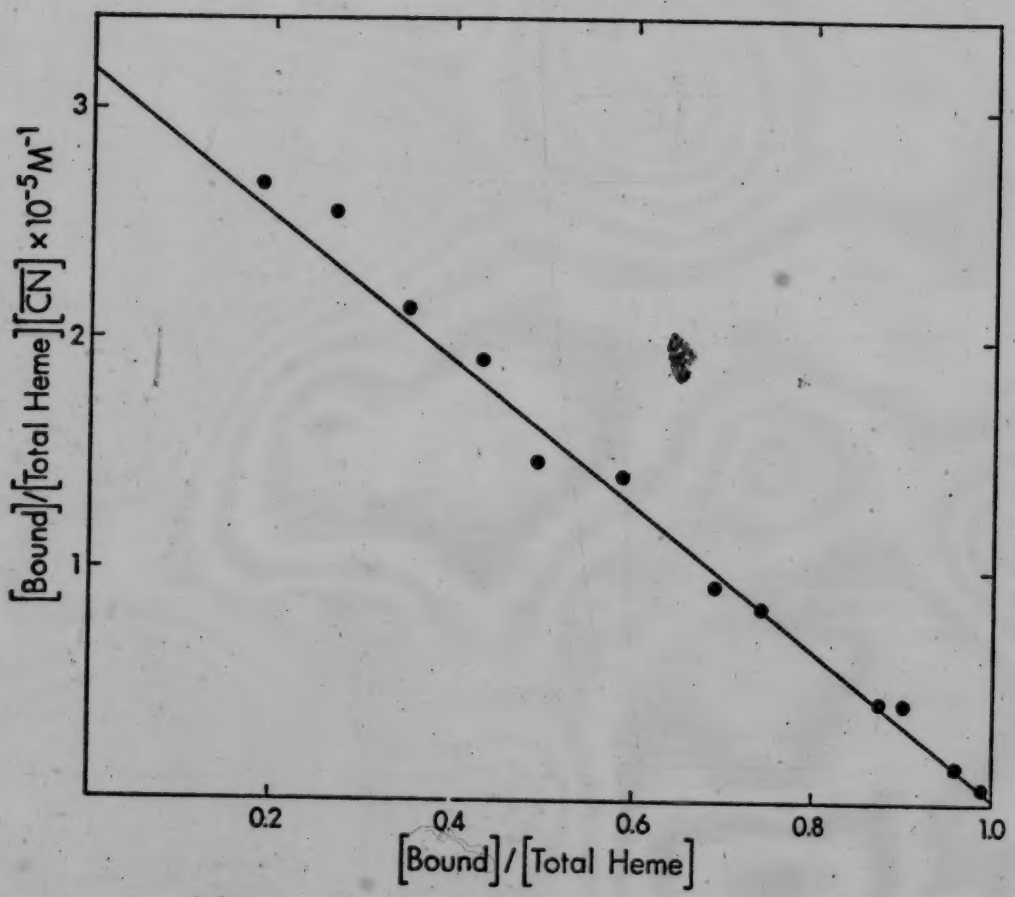

Fig. 4.1 Scatchard plot of cyanide binding to human erythrocyte catalase. Enzyme concentration 0.40 μM, pH 4.69 citrate buffer ionic strength, 0.11, 25°. [$\overline{CN}$] is the equilibrium concentration of cyanide.

Table 4.1 Data for the Binding of Cyanide by Catalase at 25°

	Experimental Rate Constants Temperature-Jump Analysis			$K_{CN} = \frac{(Fe\ CN)}{(\overline{Fe})\ (\overline{CN})}$	
pH	$k_{lapp} \times 10^{-6}$ $(M^{-1}s^{-1})$	k_{-lapp} (s^{-1})	$k_{lapp}/k_{-lapp} \times 10^{-5}$ (M^{-1})	Amplitude Data $\times 10^{-5}$ (M^{-1})	Scatchard Plot $\times 10^{-5}$ (M^{-1})
4.16					3.2 ± 0.2
4.69	1.27 ± 0.06	4.3 ± 0.4	3.0 ± 0.4	2.9 ± 0.1	3.2 ± 0.2
5.51					2.9 ± 0.4
5.70					3.1 ± 0.3
5.92	1.28 ± 0.04	4.7 ± 0.2	2.7 ± 0.2	3.2 ± 0.1	
6.58					2.8 ± 0.2
7.06	1.32 ± 0.05	4.7 ± 0.6	2.8 ± 0.4	3.1 ± 0.4	
7.56					3.4 ± 0.4
8.03					3.0 ± 0.2
8.09	1.29 ± 0.04	4.1 ± 0.4	3.1 ± 0.5	3.2 ± 0.4	
8.62					2.2 ± 0.2
8.67	0.99 ± 0.02	5.2 ± 0.2	1.9 ± 0.1	1.9 ± 0.1	
8.97					1.4 ± 0.1
9.06	0.82 ± 0.02	5.1 ± 0.3	1.6 ± 0.2	1.2 ± 0.1	1.2 ± 0.1
9.32	0.68 ± 0.04	4.5 ± 0.5	1.5 ± 0.3	1.2 ± 0.1	
9.44	0.39 ± 0.02	7.3 ± 0.4	0.53 ± 0.06	0.44 ± 0.02	
9.53					0.60 ± 0.02
9.68	0.27 ± 0.01	7.3 ± 0.1	0.37 ± 0.02	0.26 ± 0.01	
9.96	0.16 ± 0.01	7.8 ± 0.5	0.21 ± 0.03	0.13 ± 0.01	0.13 ± 0.01

Table 4.1 continued

[a]Total ionic strength = 0.11, citrate buffer pH 4.16 - 4.69, phosphate buffer pH 5.51 - 8.09, carbonate buffer pH 8.65 - 9.96.

In the temperature jump study a single relaxation process was observed under all experimental conditions (Fig. 4.2). The concentration dependence of the relaxation time, τ, at any given pH corresponds to the following simple equation:

$$Fe + CN \underset{k_{-1app}}{\overset{k_{1app}}{\rightleftharpoons}} FeCN \qquad (1)$$

and is given by (9):

$$\frac{1}{\tau} = k_{1app}\,[(\overline{Fe}) + (\overline{CN})] + k_{-1app} \qquad (2)$$

where Fe and CN represent the concentration of heme and cyanide, FeCN the heme cyanide complex and $(\overline{Fe}) + (\overline{CN})$ the equilibrium concentrations of heme and cyanide. The values of $(\overline{Fe}) + (\overline{CN})$ were calculated as previously described (10). Examples of plots of $1/\tau$ vs. $[(\overline{Fe}) + (\overline{CN})]$ are shown in (Fig. 4.3). The values of k_{1app} and k_{-1app} obtained in this manner are listed in Table 4.2.

Values of k_{1app} were also measured by means of a stopped-flow technique, (Table 4.2). The concentration dependence of the kinetics of cyanide binding is shown in Fig. 4.4. No rate saturation was observed over the concentration range 10 to 130 μM cyanide. Second-order kinetics are demonstrated by the linearity of the plots obeying the following equation:

$$k_{obs} = k_{1app}[CN] + k_{-1app} \qquad (3)$$

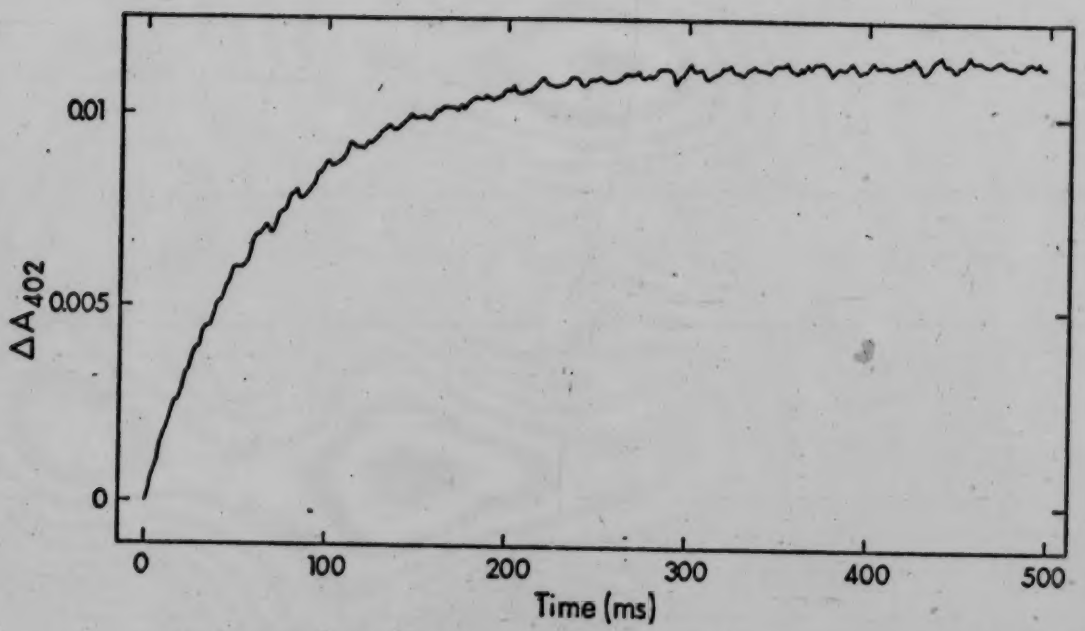

Fig. 4.2 Temperature-jump relaxation of catalase-cyanide at pH 9.06. Enzyme concentration 1.1 μM, cyanide concentration 10.9 μM, carbonate buffer ionic strength, 0.11.

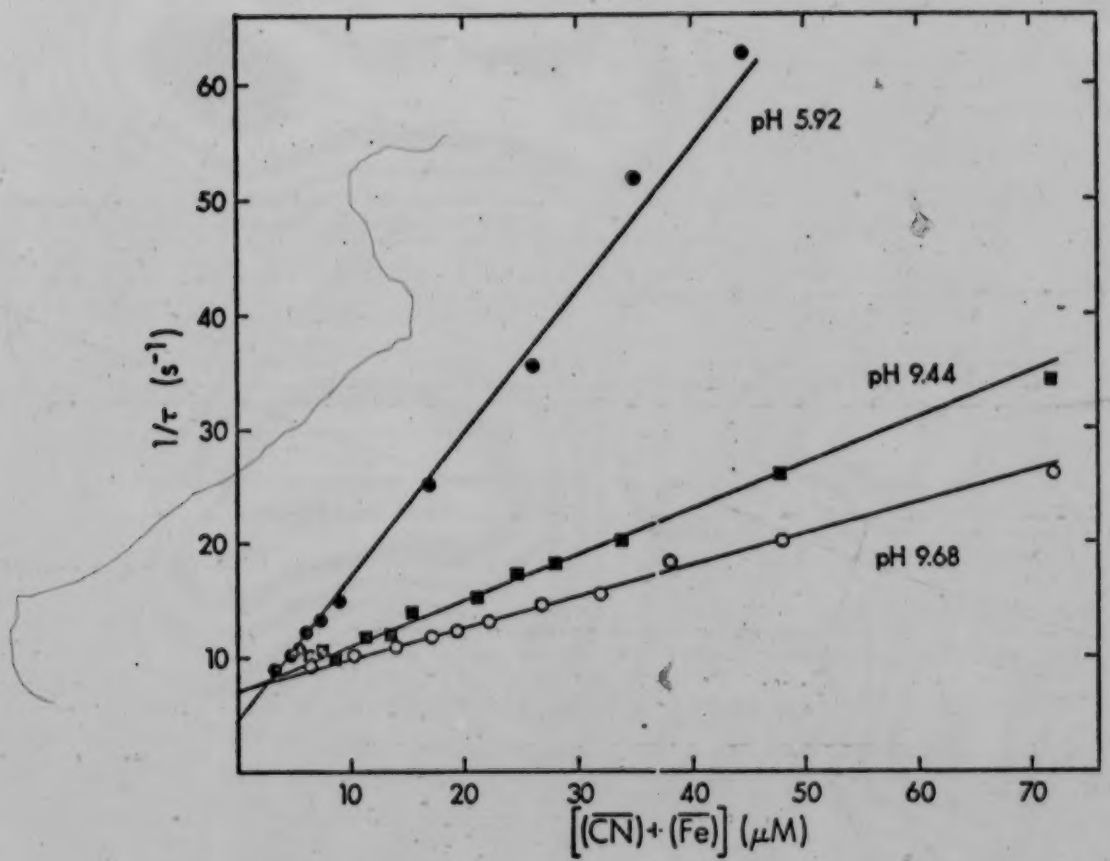

Fig. 4.3 Concentration dependence of reciprocal relaxation time against equilibrium concentration of cyanide and enzyme at various pH values. The slopes of the lines correspond to k_{1app} the second order rate constant, the intercept to k_{-1app}. Catalase concentration 0.86-0.96 μM. $[\overline{CN}]$ and $[\overline{Fe}]$ are the equilibrium concentrations of cyanide and heme respectively.

Table 4.2 Experimental Rate Constants from Stopped-Flow Data at 25°C and Ionic Strength 0.11

pH	Buffer[a]	k_{lapp} x 10^{-6} M^{-1}
4.19	Ci	1.19 ± 0.02
5.54	P	1.28 ± 0.01
6.65	P	1.34 ± 0.02
7.50	P	1.19 ± 0.01
8.65	Ca	0.97 ± 0.02
9.27	Ca	0.64 ± 0.01
9.76	Ca	0.29 ± 0.01
10.20	Ca	0.12 ± 0.01

[a]Buffer key: Ci, citrate; P, phosphate, Ca, carbonate.

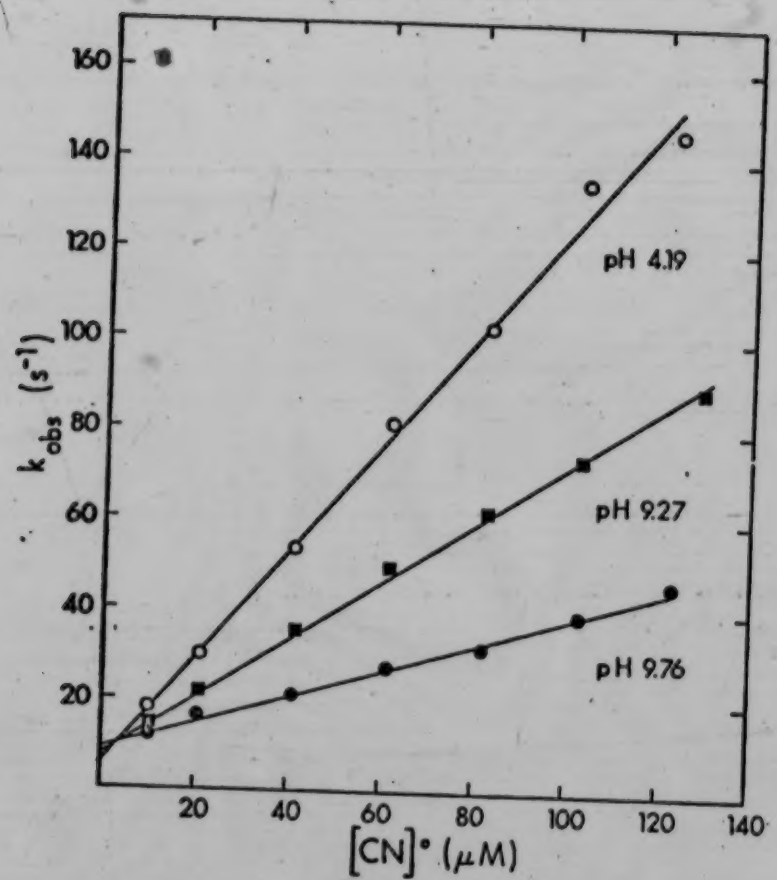

Fig. 4.4 Stopped-flow kinetics of cyanide binding to catalase at various pH values. Plots of k_{obs}, the pseudo first order rate constant for cyanide binding, as a function of total cyanide concentration $[CN]^{\circ}$. Initial catalase concentration 0.35-0.51 μM, temperature 25°, total ionic strength 0.11. The slopes of the lines correspond to k_{lapp}, the second order rate constant, and are calculated by a weighted linear least squares analysis.

Values of k_{lapp} decreased markedly with increasing pH, Fig. 4.5. The values of k_{-lapp} from stopped flow results are inaccurate due to the long extrapolation to the ordinate. The simplest scheme which accounts for the k_{lapp} values is:

$$\begin{array}{ccc} Fe + HCN & \xrightarrow{k_1} & FeCN \\ & H^+ \rightleftharpoons K_a & \\ & CN^- & \end{array} \qquad (4)$$

where K_a is the dissociation constant for hydrocyanic acid and k_1 is the pH independent rate constant for the reaction of catalase and cyanide. The apparent second order rate constant, k_{lapp} is given by:

$$k_{lapp} = \frac{k_1}{1 + \frac{K_a}{[H^+]}} \qquad (5)$$

Analysis of the k_{lapp} vs. pH rate profile using a non-linear least squares program (11) give values of pK_a 9.20 ± 0.05 and $k_1 = (1.3 \pm 0.1) \times 10^6\ M^{-1}s^{-1}$.

The value of k_{-lapp} increased with increasing pH (Fig. 4.6). The simplest scheme which accounts for the k_{-lapp} data is:

$$\begin{array}{lll} & \xrightarrow{k_{-1}} & Fe + HCN \\ H\,Fe\,CN & & \\ & \xrightarrow{k_{-2}[OH^-]} & Fe + CN^- + H_2O \end{array} \qquad (7)$$

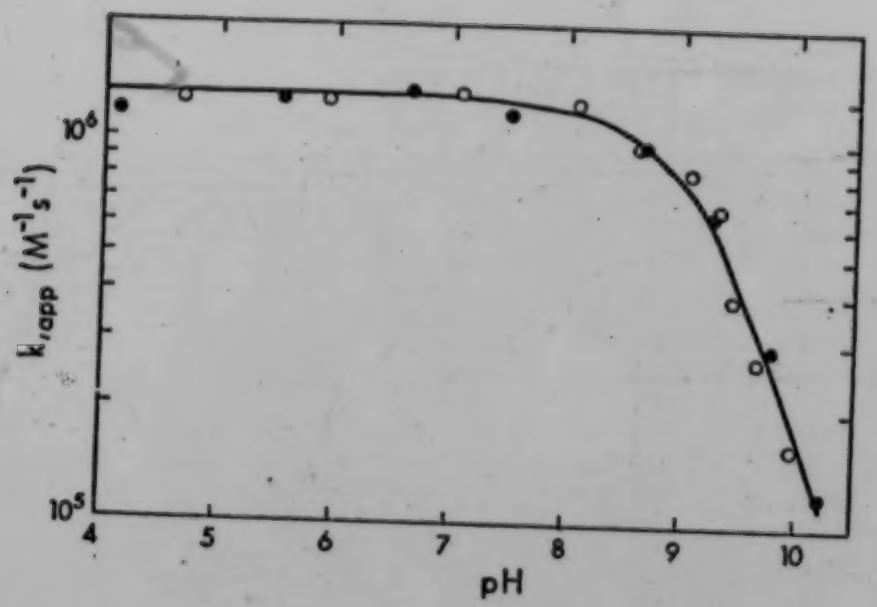

Fig. 4.5 The pH dependence of k_{1app}. The best line through the data was calculated using a non-linear least squares analysis of Equation 5. ●, stopped flow data; ○ temperature jump data.

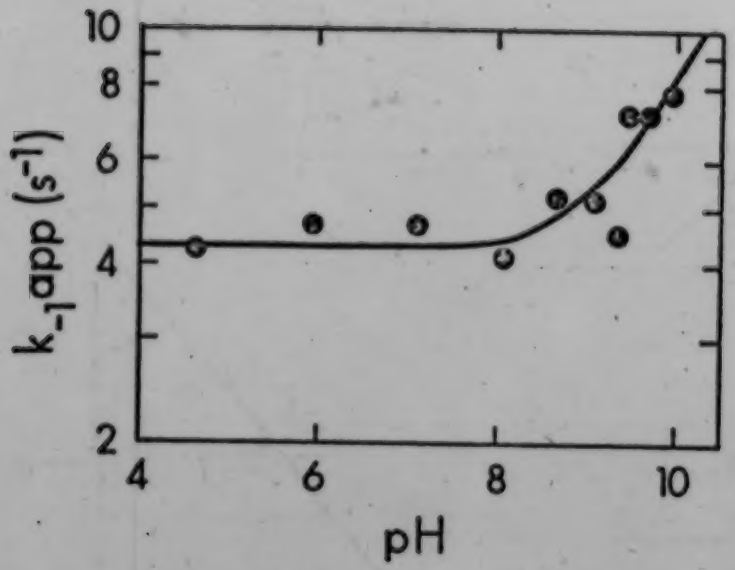

Fig. 4.6 The pH dependence of k_{-1app}. The best fit line through the data was calculated using a non-linear least squares analysis of Equation 8.

where k_{-1} and k_{-2} are pH independent dissociation rate constants. The apparent dissociation constant k_{-1app} is given by

$$k_{-1app} = k_{-1} + k_{-2}[OH^-] \qquad (8)$$

A nonlinear least squares analysis of k_{-1app} versus pH profile (Fig. 4.6) yielded the best fit parameters listed in Table 4.3.

In a temperature jump experiment the relaxation amplitudes are functions of reaction enthalpies and extinction coefficients and can be used to determine equilibrium constants. For the formation of a 1:1 complex

$$Fe + CN \underset{k_{-1}}{\overset{k_1}{\rightleftharpoons}} FeCN \qquad (9)$$

the amplitude (δA) of the relaxation is given by equation 10 (12-15)

$$\delta A = \ell \Delta\varepsilon \left(\frac{\Delta H^\circ}{RT^2} \delta T \right) \Gamma \qquad (10)$$

where ΔH° is the intrinsic reaction enthalpy, $\Delta\varepsilon$ the difference in molar extinction coefficients, δT is the temperature change, ℓ the optical path length and Γ is the amplitude factor.

Table 4.3 Parameters Obtained from Analysis of k_{lapp}, k_{-lapp} and K_{CN} versus pH Profiles for Cyanide Binding to Catalase

Parameter	Numerical Value[a]		
	k_{lapp} analysis	k_{-lapp} analysis	K_{CN} analysis
$k_1 \times 10^{-6}$ $(M^{-1}s^{-1})$	1.3 ± 0.1		1.4 ± 0.1
k_{-1} (s^{-1})		4.6 ± 0.3	4.4 ± .3
$k_2 \times 10^{-5}$ $(M^{-2}s^{-1})$			4.7
$k_2' \times 10^{-3}$ $(M^{-1}s^{-1})$	negligible		8
$k_{-2} \times 10^{-5}$ $(M^{-1}s^{-1})$		0.5 ± 0.1	1.0 ± 0.6
pK_a	9.2 ± 0.05		9.2 ± 0.1

[a]Errors estimated from the standard deviations of the non-linear least squares fits.

The amplitude factor can be expressed as:

$$\Gamma = \frac{(\overline{Fe})(\overline{CN})}{(\overline{Fe}) + (\overline{CN}) + K_{CN}^{-1}} \qquad (11)$$

$$= \frac{1}{2K_{CN}} \{[1 - 4(Fe)^{\circ}(CN)^{\circ}/((Fe)^{\circ} + (CN)^{\circ} + K_{CN}^{-1})^2]^{\frac{1}{2}} - 1\} \qquad (12)$$

where the superscript $^{\circ}$ refers to initial concentrations of heme and cyanide. Equation 10 can be rewritten as

$$\Delta OD = \ell \Delta\varepsilon \frac{\Delta K}{K} \Gamma \qquad (13)$$

for finite but small changes in K ($\Delta K << K$).

Since ℓ, $\Delta\varepsilon$, and $\Delta K/K$ are constants, the shape of the experimental curve ΔOD versus $(CN)^{\circ}/(Fe)^{\circ}$ will be the same as that of Γ versus $(CN)^{\circ}/(Fe)^{\circ}$. By using a non-linear least squares program the experimental points can be fitted to find the best statistical value of the equilibrium constant. An asymmetric bell shaped curve is found for a plot of ΔOD vs. $(CN)^{\circ}/(Fe)^{\circ}$ (Fig. 4.7). The solid line represents the best value of the association constant K_{CN} calculated for the curve and is $(2.9 \pm 0.1) \times 10^5\ M^{-1}$. A scale factor was included in the curve fitting program to superimpose the theoretical curve predicted from Γ versus initial concentrations on the experimental points (15). The values of K_{CN} calculated from amplitude measurements and from temperature jump kinetic data k_{1app}/k_{-1app},

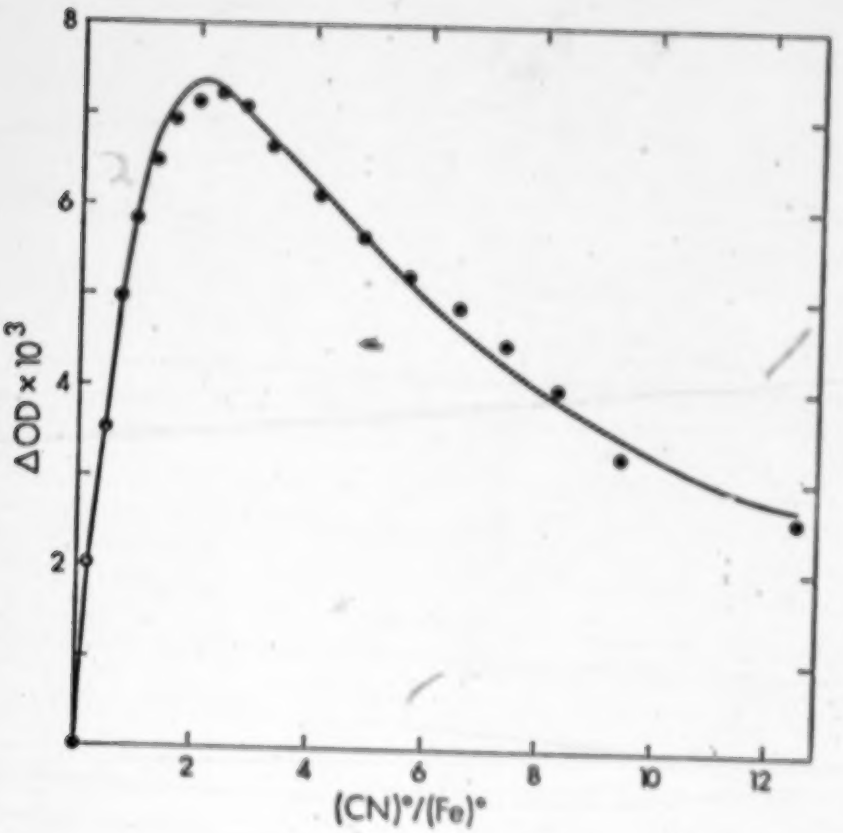

Fig. 4.7 Relaxation amplitudes as a function of total cyanide, $(CN)^{o}$. The heme concentration $(Fe)^{o}$ was 3.2 μM. The curve represents the best non-linear least squares fit of the data to Equation 12. Experimental conditions, pH 4.69 citrate buffer, ionic strength, 0.11, final temperature 25°.

are shown in Table 4.1. In the absence of ligand there were no detectable absorbance changes due to a temperature jump of 2.8° of the enzyme in aqueous solution over the time span of 1 to 1000 ms. Specific buffer effects on the relaxation amplitudes were checked by measuring ΔOD at maximum values of $(CN)^{o}/(Fe)^{o}$, keeping the ionic strength constant at 0.22 and varying the proportions of K_2SO_4 and buffer components. The relaxation amplitudes were identical for phosphate, citrate and carbonate buffers when the contribution of K_2SO_4 to the total ionic strength ranged from 0 to 0.15.

The equilibrium constant K_{CN} determined by all methods decreased with increasing pH (Fig. 4.8). In the pH independent region the value of K_{CN} calculated by averaging the values from all methods is $(3.1 \pm 0.2) \times 10^5\ M^{-1}$. The dissociation rate constant of the catalase cyanide complex k_{-1} in this pH region is $4.2 \pm 0.6\ s^{-1}$.

The simplest mechanism to explain the pH dependence of values is

$$\begin{array}{ccc} Fe + HCN & \overset{k_1}{\underset{k_{-1}}{\rightleftharpoons}} & H\,Fe\,CN \\ \Big\| H^+ \\ \Big\| K_a \\ Fe + CN^- + H_2O & \overset{k_{-2}[OH^-]}{\underset{k_2}{\rightleftharpoons}} & \end{array} \qquad (14)$$

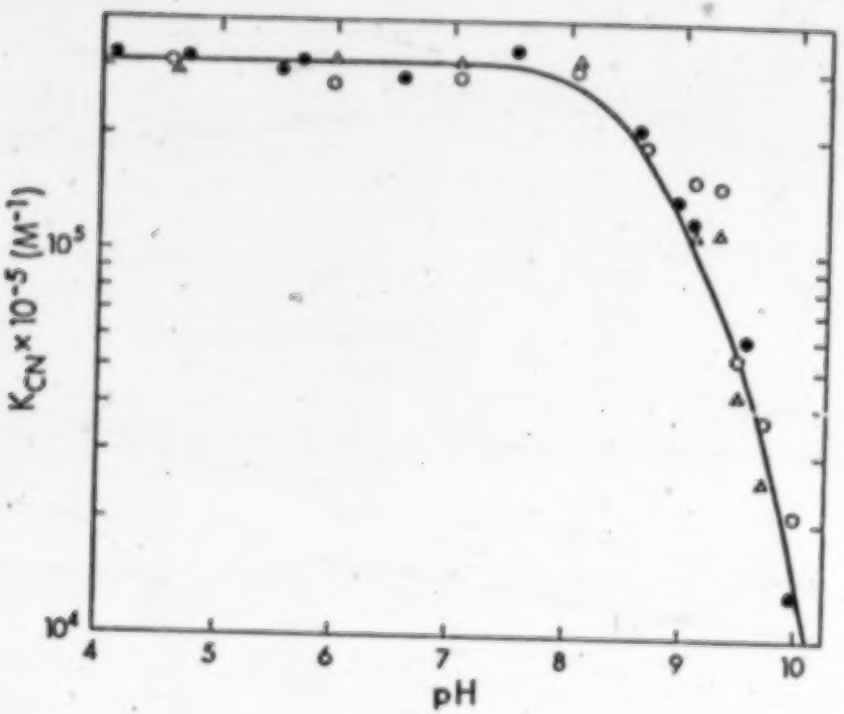

Fig. 4.8 The pH dependencd of K_{CN}. The best line through the data was calculated using a non-linear least squares analysis of Equation 15. O kinetic determination, Δ relaxation amplitude data, ●, Scatchard data.

The value of k_2 is assumed to be small as shown in k_{1app} analysis. The above scheme (14) for cyanide binding predicts

$$K_{CN} = \frac{k_1}{\dfrac{1 + \dfrac{K_a}{[H^+]}}{k_{-1} + k_{-2}[OH^-]}} \qquad (15)$$

Analysis of the K_{CN} versus pH profile yielded the parameters listed in Table 4.3. By applying the principle of detailed balancing k_2 is approximately 4.7×10^5 $M^{-2}s^{-1}$ and k_2' the second order rate constant for the reaction of dissociated cyanide and catalase is 8×10^3 $M^{-1}s^{-1}$ in agreement with the experimental data.

4.5 Discussion

The values of the equilibrium constant determined spectrophotometrically and from temperature jump data are comparable. In the pH independent region a value of $(3.1 \pm 0.2) \times 10^5$ M^{-1} was found. This result is similar to a value of 2.8×10^5 M^{-1} reported in an early kinetic study (16) where k_1 at pH 7.0 was 9×10^5 $M^{-1}s^{-1}$ and k_{-1} 3.2 s^{-1} for horse liver catalase but is higher than the value later reported for human and horse erythrocyte catalase, $K_{diss} = 7 \times 10^{-6}$, and 4×10^{-6} respectively (2). In all earlier studies an increase in K_{diss} as a function of pH not attributable to the dissociation of hydrocyanic

acid alone was observed. This can now be explained by an increase in k_{-1app} as observed in the present study.

Curvature in a Scatchard plot is an indication of cooperative effects in a binding reaction. The straight lines obtained in the Scatchard plots for cyanide binding to catalase indicate the four heme groups act independently. The pK for the dissociation of hydrocyanic acid is 9.0 at 25° and an ionic strength of 0.11 (17). Analysis of the k_{1app} kinetic data and K_{CN} equilibrium data yields a group with a pK_a of 9.2 that affects the association reaction, when this group is deprotonated the reaction slows. Thus the formation of the cyanide complex seems to be by reaction of catalase with unionized hydrocyanic acid just as compound I formation required the unionized form of hydroperoxides (1). The participation of the undissociated acid rather than the conjugate base in the rate limiting step of the reaction does not necessarily imply that the protonated acid is ligated in the complex. Evidence from inorganic chemistry indicates that transition metals do not bind the neutral form of ligands such as cyanide (18), and although it cannot be proven the evidence above suggests it is the neutral form of cyanide which binds preferentially. Upon binding the proton could be picked up by an exposed group on the protein (19). The equilibrium analysis also agrees with the observation that cyanide binding to catalase occurs with no net uptake or loss of

protons to the medium (20).

The dissociation curve, k_{-1app} versus pH can be fit to an equation where k_{-2} is the dissociation of FeCN:

$$\begin{array}{ccc} \text{H Fe CN} & \xrightarrow{k_{-1}} & \text{Fe + HCN} \\ {\scriptstyle H^+}\uparrow\downarrow K_{CN} & & \\ \text{FeCN} & \xrightarrow{k_{-2}} & \text{Fe + CN}^- \end{array} \qquad (16)$$

This would lead to the equilibrium mechanism below:

$$\begin{array}{ccc} \text{Fe + HCN} & \underset{k_{-1}}{\overset{k_1}{\rightleftharpoons}} & \text{H Fe CN} \\ {\scriptstyle H^+}\uparrow\downarrow K_a & & {\scriptstyle H^+}\uparrow\downarrow K_e \\ \text{Fe + CN} & \underset{k_{-2}}{\overset{k_2}{\rightleftharpoons}} & \text{FeCN} \end{array}$$

This mechanism is invalid since parameters from this curve fitting predict that k_2, the reaction of ionized cyanide and catalase, is approximately the same magnitude as k_1.

The pH dependence of the dissociation rate is unusual. Eqs. 7 and 14 predict that the increase in the reverse rate as pH increases is due to the contribution of k_{-2}.

4.6 References

1. Palcic, M.M. and Dunford, H.B. (1980) J. Biol. Chem. in press.
2. Chance, B. (1952) J. Biol. Chem. 194, 483-496.
3. Palcic, M.M. and Dunford, H.B. (1979) Can. J. Biochem. 57, 321-329.
4. Bonaventura, J., Schroeder, W.A. and Fang, S. (1972) Arch. Biochem. Biophys. 150, 606-617.
5. Ryan, J.A. and Culshaw, G.W. (1944) Analyst 69, 370-371.
6. Long, C., King, E.J. and Sperry, W.M. (1968) Biochemist's Handbook pp. 29-42, Spon, London.
7. Roman, R., Dunford, H.B. and Evett, M. (1971) Can. J. Chem. 49, 3059-3063.
8. Scatchard, G. (1949) Ann. N.Y. Acad. Sci. 51, 660-672.
9. Eigen, M. and de Maeyer, L. (1963) in Technique in Organic Chemistry, Part II, Vol. VII (Weissburger A., ed.) 2nd ed. pp. 895-1054. Interscience, New York.
10. Dolman, D., Dunford, H.B., Chowdhury, D.M. and Morrison, M. (1968) Biochemistry 7, 3991-3996.
11. Hasinoff, B.B. and Dunford, H.B. (1970) Biochemistry 9, 4930-4939.
12. Winkler-Oswatitsch, R. and Eigen, M. (1979) Angew. Chem. Int. Ed. Engl. 18, 20-49.
13. Thusius, D., Blazy, B. and Baudras, A. (1976) Biochemistry 15, 250-256.
14. Chock, P.B. (1971) Biochimfe 53, 161-172.

15. Bernasconi, C.F. (1976) Relaxation Kinetics pp. 85-97.

16. Chance, B. (1949) J. Biol. Chem. 179, 1299-1309.

17. Ellis, W.D. and Dunford, H.B. (1968) Biochemistry 7, 2054-2062.

18. Jones, L.H. (1963) Inorg. Chem. 2, 777-780.

19. George, P. and Lyster, R.L.J. (1958) Proc. Nat. Acad. Sci. U.S.A. 44, 1013-1029.

20. Schonbaum, G.R. and Chance, B. (1976) in The Enzymes (Boyer, P.D. ed.) Vol. 13, Part C. pp. 363-408, Academic Press, New York.

4.7 Acknowledgments

I would like to thank Dr. T. Araiso for helpful discussions during this work and Ms. I.M. Ralston for assistance with the computer analysis.

APPENDIX I.

CARBOXYPEPTIDASE A

Introduction

An objective of research in this laboratory is to attempt to elucidate the common features of the mechanisms of action of different enzymes. Although this is a long term goal which is at present nowhere near attainment, this appendix is devoted to summarizing the present state of knowledge of a well studied metalloenzyme, carboxypeptidase A.

Carboxypeptidase A is an exopeptidase, removing the C-terminal amino groups from polypeptides, specific for large hydrophobic amino acids such as phenylalanine. The closely related carboxypeptidase B specifically removes lysine and arginine residues. Carboxypeptidase A contains one atom of zinc bound to a single polypeptide chain. The most studied type is the bovine pancreatic enzyme first isolated by Waldschmidt-Leitz and Purr in 1929 (1). The enzyme was crystallized by Annon in 1937 (2) and the sequence was determined by Neurath and co-workers in 1969 (3). The enzyme has 307 amino acid residues and a molecular weight of 34,472. The X-ray structure at 2 Å resolution was determined in 1967 by Lipscomb and coworkers (4). The molecule contains 38% α-helical structure and 17% β-sheet (4). At an ionic strength of 0.2 the

isoelectric point is 6.0 (5). The molar extinction coefficient at 270 nm is 6.42×10^4 $M^{-1}cm^{-1}$ (5).

The enzyme is secreted by the acinar cells of the pancreas as a zymogen procarboxypeptidase A. The zymogen is activated by the removal of a peptide of about 64 residues from the N-terminus by trypsin. The zymogen has significant catalytic activity. Carboxypeptidase A is commercially available and an isolation procedure using affinity chromatography has been described recently (6).

Catalytic Activity

Carboxypeptidase removes the C-terminal amino acids from a peptide chain if the C-terminal carboxylate group is free.

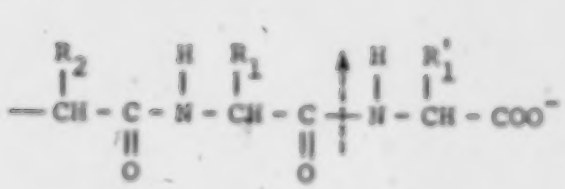

(1)

All R_1' amino acids are hydrolyzed but lysine, arginine and proline. The hydrolysis is most rapid when R_1' is a neutral aromatic or branched aliphatic residue, i.e., hydrophobic. Dipeptides with a free amino group are hydrolyzed slowly but if this group is blocked by N-acylation, the hydrolysis is rapid. Studies of longer polypeptides indicate that the nature of the side chains of at least five residues influence K_m and k_{cat} to some extent (7). Ester bonds in a series of synthetic esters are also hydrolyzed.

Substrates used for standard assay are carbobenzoxyglycl-L-phenylalanine [CGP] (A) and hippuryl-L-phenyalanine [HPLA] (B). The change in absorbance at 254 nm is monitored as the substrates are hydrolyzed.

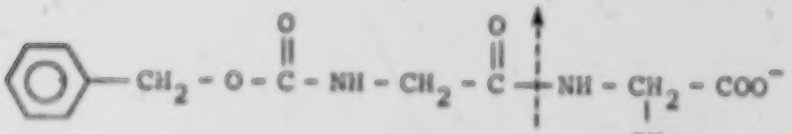

[CGP] (A)

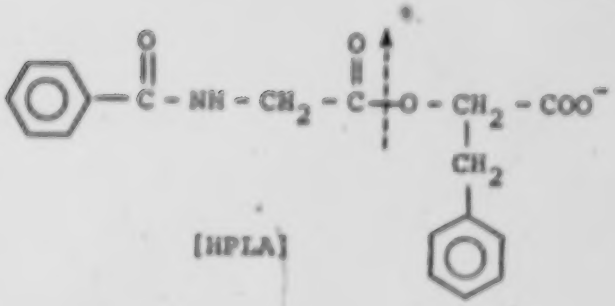

[HPLA] (B)

X-Ray Structure

The zinc atom is coordinated to three groups, glutamic acid 72, histidine 196 and histidine 69 . Water completes a distorted tetrahedron. In 20% of the molecules, the phenolic oxygen of tyrosine-248 is a fourth ligand (8); the side chain of this residue is very mobile. The X-ray structure of a complex of the enzyme with the dipeptide glycyl-L-tyrosine which is hydrolyzed very slowly has also been determined at 2 Å resolution (8). The binding features are (Fig. 5.1) :

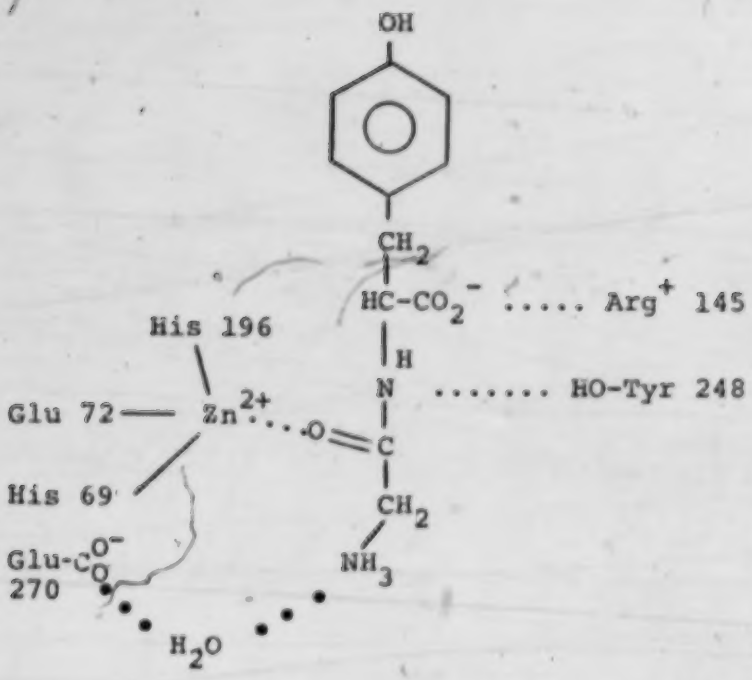

Fig. 5.1 The (partly) non-productively bound complex of a dipeptide and carboxypeptidase A (8).

i) the aromatic side chain binds in a hydrophobic binding pocket that contains no specific binding groups and is large enough to accommodate a tryptophan side chain

ii) the terminal carboxyl group of the substrate (which is essential for cleavage) interacts with the positively charged guanidinium group of arginine 145

iii) the carbonyl oxygen of the peptide group susceptible to hydrolysis replaces the water molecule at the fourth coordination position of zinc

iv) the phenolic oxygen of tyrosine-248 is within 3 Å of the scissile bond

v) only in dipeptides does glutamic acid 270 bind through water to the α-amino group

Reaction Mechanism

A metal ion is needed for activity and replacement of zinc by other metals changes enzymic efficiency, Table 5.1 (9). Analysis of the kinetic data is complicated by substrate inhibition and product inhibition and activation. The rate *vs.* pH profiles follow a bell shaped curve with an optimum at pH 7.5 (10,11). Analysis of the profiles yield two enzyme pK_a's, the first 6.5 ± 0.4 and the second varies from 9.4 to 7.5. Enthalpies of ionization are 3.1 kcal/mole for the group with a pK_a 6.5 and 5.4 kcal/mole for the second enzyme pK_a (12). The lower pK_a may be glutamic

Table 5.1 Activity of Metallocarboxypeptidases.[a]

Element	Peptidase Activity	Esterase Activity
Zn	100	100
Co	160	95
Ni	106	87
Mn	8	35
Cu	0	0
Hg	0	116
Cd	0	150
Pb	0	52

[a]Activity toward N-carbobenzoxyglycyl-L-phenylalanine (peptidase) and O-hippurlyl-L-β-phenyllactate (esterase) at pH 7.5.

acid 270 needed in its carboxylate form for activity although arguments have been raised that a conformation change of the enzyme may be responsible for the loss of activity as pH decreases (13). The higher pK_a group has not been assigned unambiguously. It may be the ionization of the metal water complex or the phenolic hydroxyl of tyrosine 248 since acetylation of this group abolishes peptide hydrolysis and the hydrolysis of certain esters.

Two classes of mechanisms are suggested, based on X-ray and enzyme modification work. In one case glutamic acid 270 acts as a nucleophile at the scissile carbonyl. This mechanism would lead to an anhydride acyl-enzyme intermediate temporarily attached to glutamate 270 (Scheme 1). In the second type of mechanism the carboxylate of glutamate 270 acts as a general base delivering a water molecule to the scissile carbonyl (Scheme 2). Evidence for the acyl intermediate comes from a study using the ester substrate O-(trans-ρ-chlorocinnamoyl)-L-β-phenyllactate

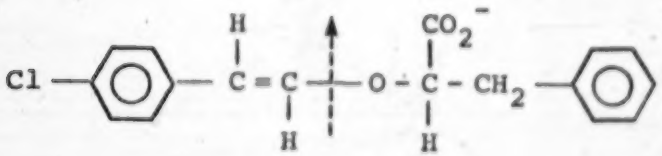

The reaction was monitored by changes in the spectrum of the cinnamoyl group and at low temperatures a biphasic reaction was seen in the presence of excess enzyme (14,15).

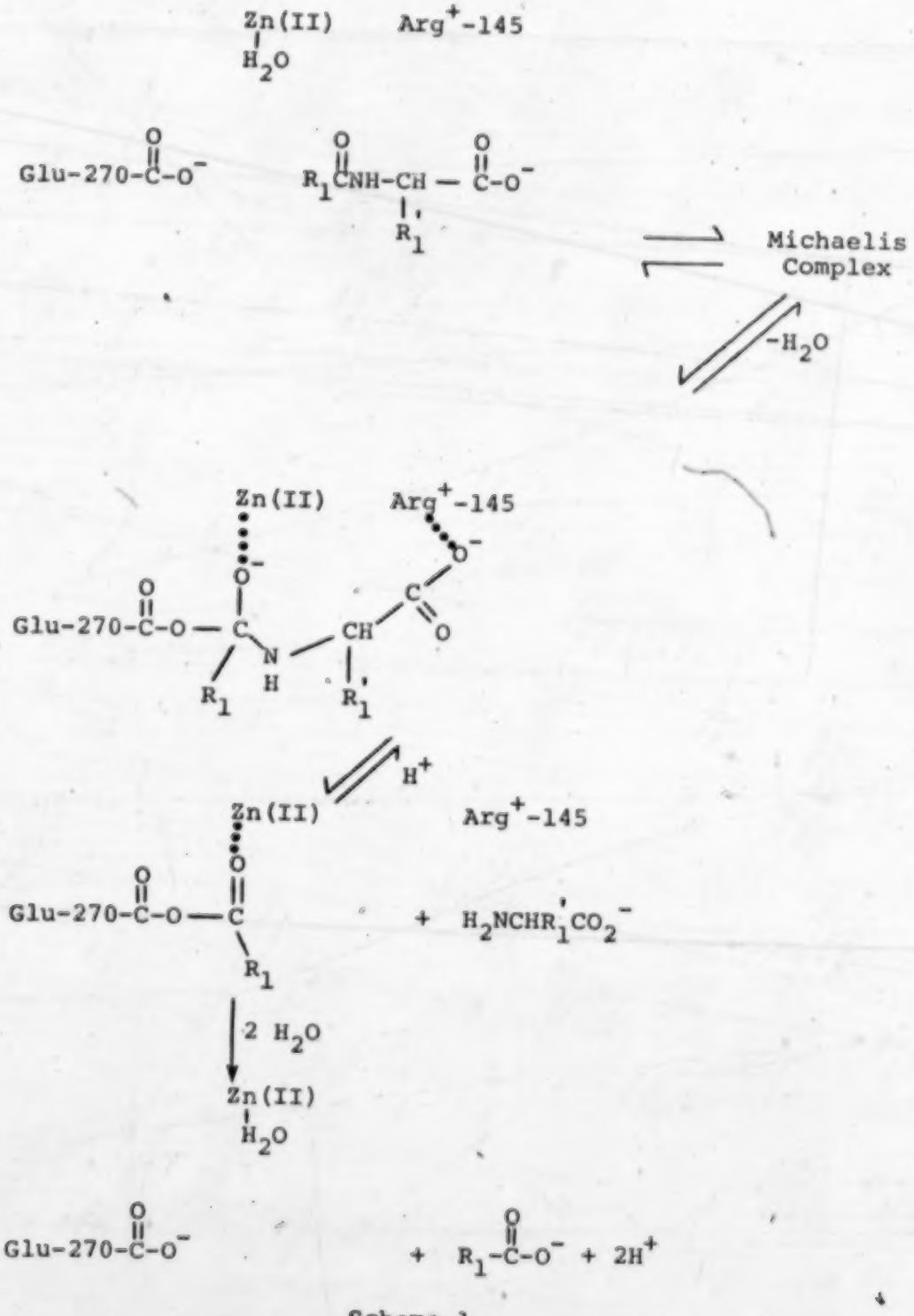
Zn(II)
H2O
Arg+-145
Glu-270-C-O-
R1CNH-CH-C-O-
R1'
Michaelis Complex
-H2O
Zn(II)
Arg+-145
Glu-270-C-O-
H+
Zn(II)
Arg+-145
Glu-270-C-O-
+ H2NCHR1'CO2-
2 H2O
Zn(II)
H2O
Glu-270-C-O-
+ R1-C-O- + 2H+

Scheme 1.

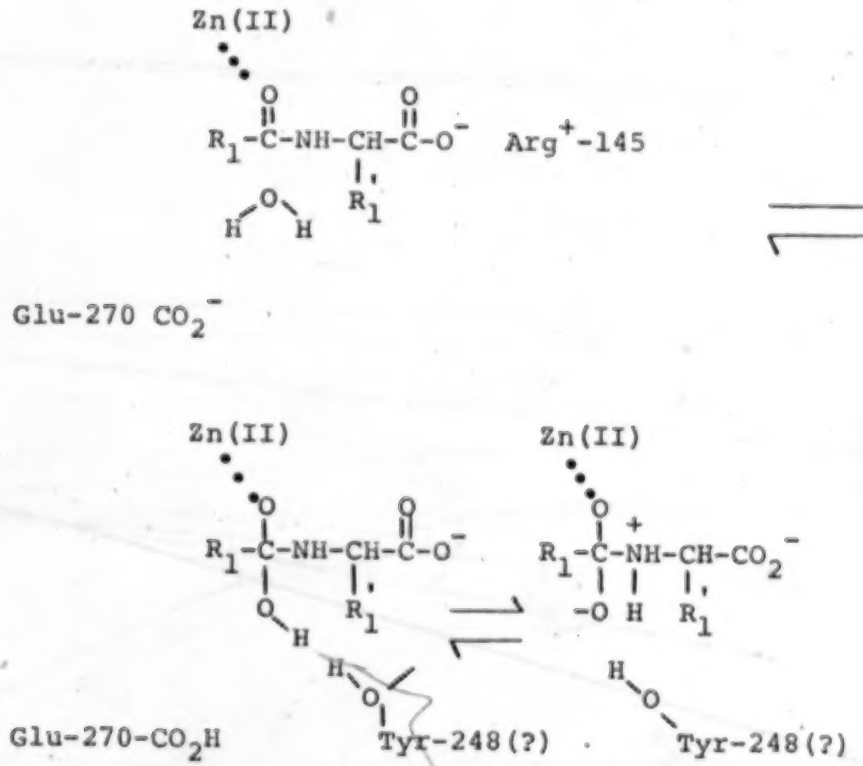
Zn(II)
Arg+-145
Glu-270 CO2-
Zn(II)
Zn(II)
Glu-270-CO2H
Tyr-248(?)
Tyr-248(?)
Zn(II)
+ H2NCHCO2- + H2O
Zn(II)
H2O
+

Scheme 2.

At higher temperatures the rate constant for the second phase increased more rapidly than for the first phase. The two phases were interpreted as being the formation and hydrolysis of an acyl-enzyme. Further evidence for this mechanism was shown at -58° where the acyl-enzyme is stable. A strongly binding competitive inhibitor of the enzyme L-benzylsuccinate did not displace the cinnamoyl group, indicating it is covalently bound.

Evidence for the second, general base mechanism comes from oxygen-18 exchange measurements (16). If hydrolysis occurs by the anhydride route then the synthesis of a peptide in the reverse reaction requires the initial formation of the anhydride from enzyme and RCO_2^-.

$$RC^{18}O_2^- + E-CO_2^- \xrightarrow[H_2{}^{18}O]{} E-CO_2{}^{18}OCR$$

$$\xrightarrow[H_2O]{} RCOO^{18}O^- + E-CO_2$$

This would lead to exchange of ^{18}O between the substrate and water. However exchange does not occur unless a free amino acid $NH_3^+CH(R')CO_2^-$, R' = phenylalanine or leucine, is added. It may be that esters are hydrolyzed by the nucleophilic attack mechanism and peptides by a general base mechanism (17). It is not improbable that the mechanisms

are different because chemical modification of the enzyme or replacement of the metal ion affects esterase and peptidase activities in different ways.

2.5 References

1. Waldschmidt-Leitz, E. and Purr, A. (1929) Ber. Deut. Chem. Ges. 62, 2217-2226.
2. Anson, M.L. (1937) J. Gen. Physiol. 20, 663-669.
3. Bradshaw, R.A., Ericsson, L.H., Walsh, K.A. and Neurath, H. (1969) Proc. Natl. Acad. Sci. U.S. 63, 1389-1394.
4. Reeke, G.N., Hartsuck, J.A., Ludwig, M.L., Quiocho, F.A., Steitz, T.A. and Lipscomb, W.N. (1967) Proc. Natl. Acad. Sci. U.S. 58, 2220-2226.
5. Quiocho, F.A. and Lipscomb, W.N. (1971) Adv. Prot. Chem. 25, 1-78.
6. Bazzone, T.J., Sokolovsky, M., Cueni, L.B. and Vallee, B. (1979) Biochemistry 18, 4362-4366.
7. Abramowitz, N., Schechter, I. and Berger, A. (1967) Biochem. Biophys. Res. Commun. 29, 862-867.
8. Lipscomb, W.N., Hartsuck, J.A., Quiocho, F.A. and Reeke, G.N. (1969) Proc. Natl. Acad. Sci. U.S. 64,28-35.
9. Lipscomb. W.N. (1973) Proc. Natl. Acad. Sci. U.S. 70, 3797-3801.
10. Auld, D.S. and Vallee, B.L. (1970) Biochemistry 9, 4352-4359.

11. Carson, F.W. and Kaiser, E.T. (1966) J. Amer. Chem. Soc. 88, 1212-1223.

12. Auld, D.S. and Vallee, B.L. (1971) Biochemistry 10, 2892-2897.

13. Bunting, J.W. and Chu, S.S.-T. (1976) Biochemistry 15, 3237-3244.

14. Kaiser, E.T. and Kaiser, B.L. (1972) Acc. Chem. Res. 5, 219-224.

15. Makinen, M.W., Yamamura, K. and Kaiser, E.T. (1976) Proc. Natl. Acad. Sci. U.S. 3882-3886.

16. Breslow, R. and Wernick, D. (1976) J. Amer. Chem. Soc. 98, 259-261.

17. Breslow, R. and Wernick, D. (1977) Proc. Natl. Acad. Sci. 74, 1303-1307.